Engineering Holographic Phase Diagrams with Dome

Presented by **Yun-Long Zhang (张云龙)**

based on the work with Jiunn-Wei Chen, Shou-Huang Dai, Debaprasad Maity,

arXiv: 1603.08259

Department of Physics, National Taiwan University

— zhangyunlong001@gmail.com 2016-08-29 @ APCTP

Outline

1. Holographic Properties of Black Hole

2. Engineering Holographic Phase Diagrams

3. Discussion and Outlook

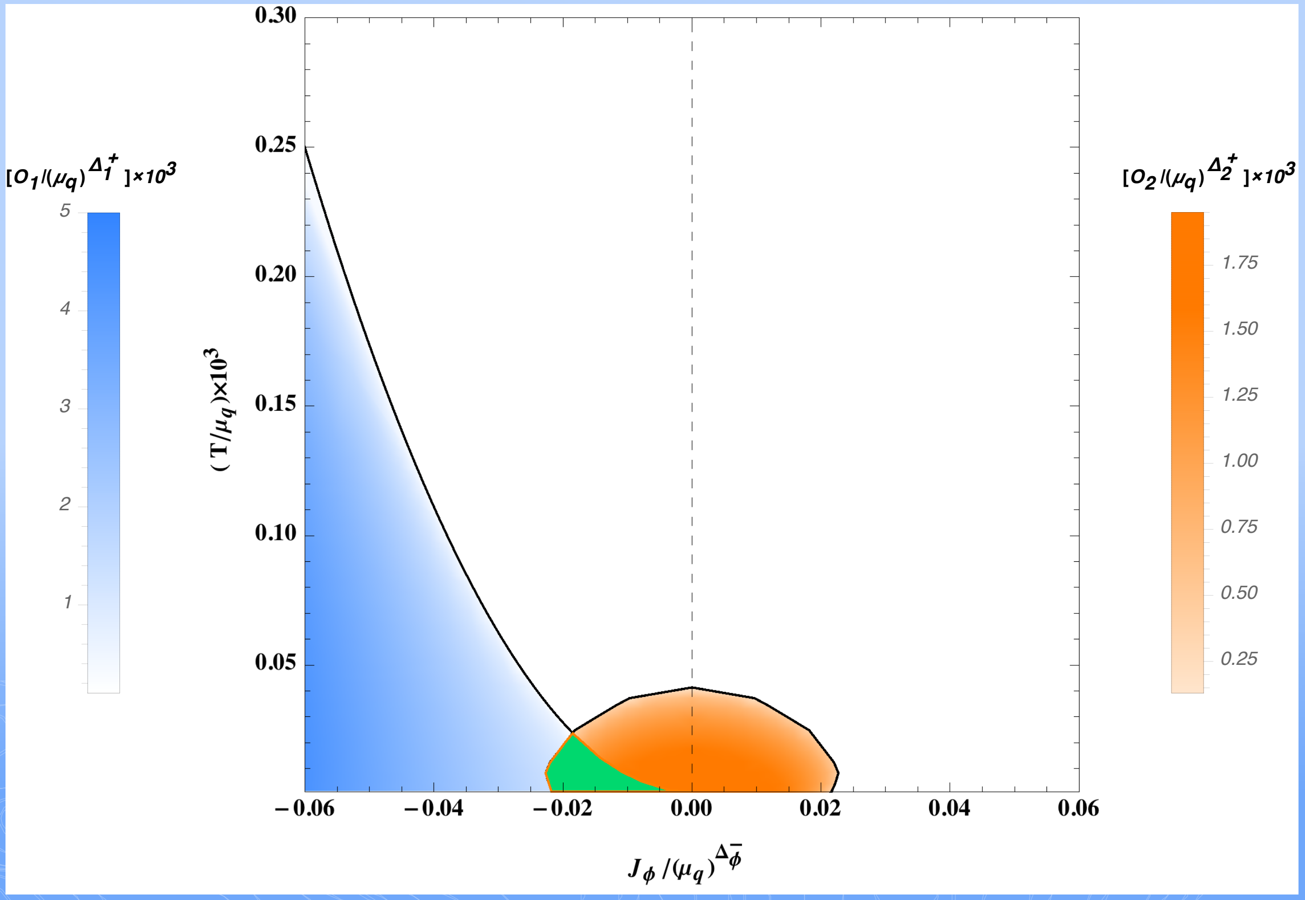

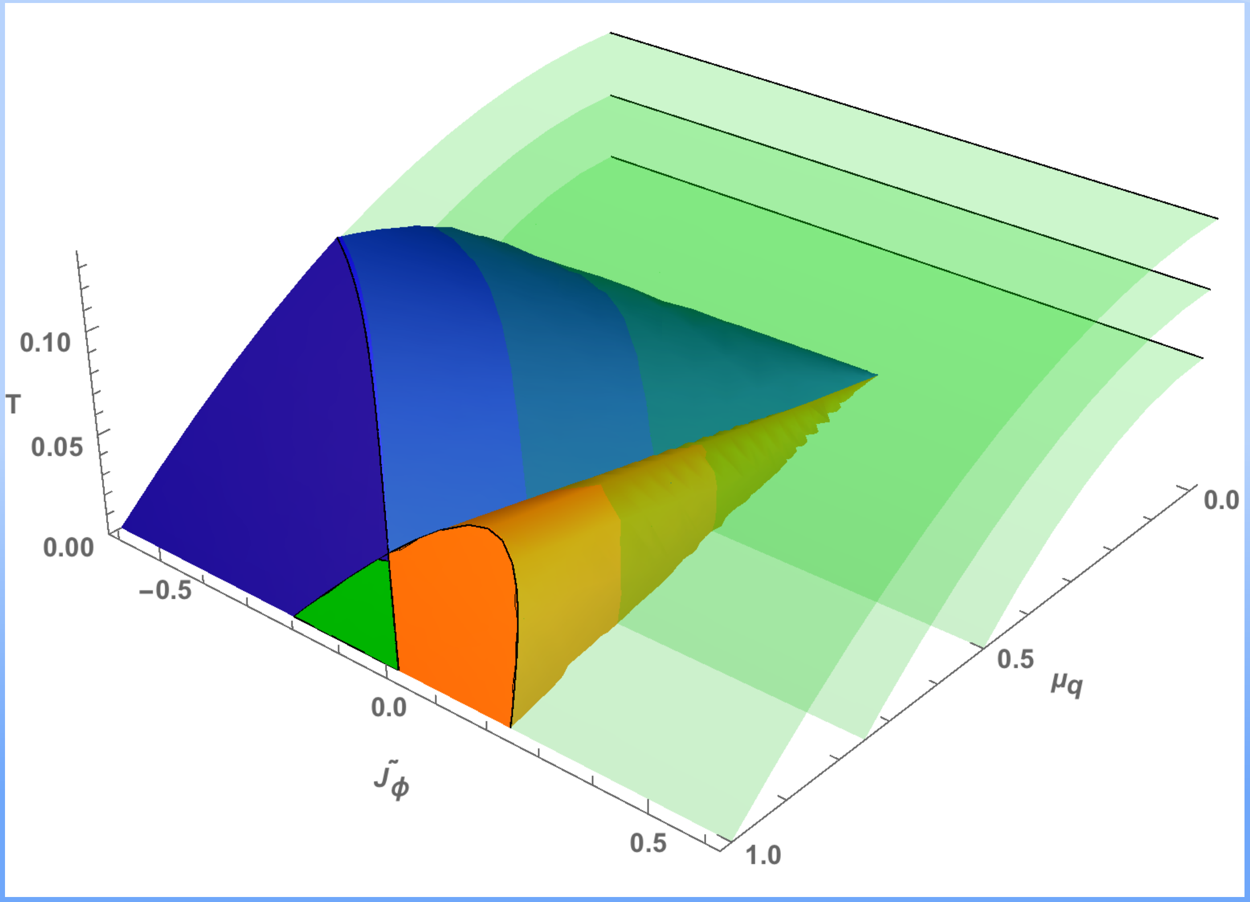

Holographic Properties

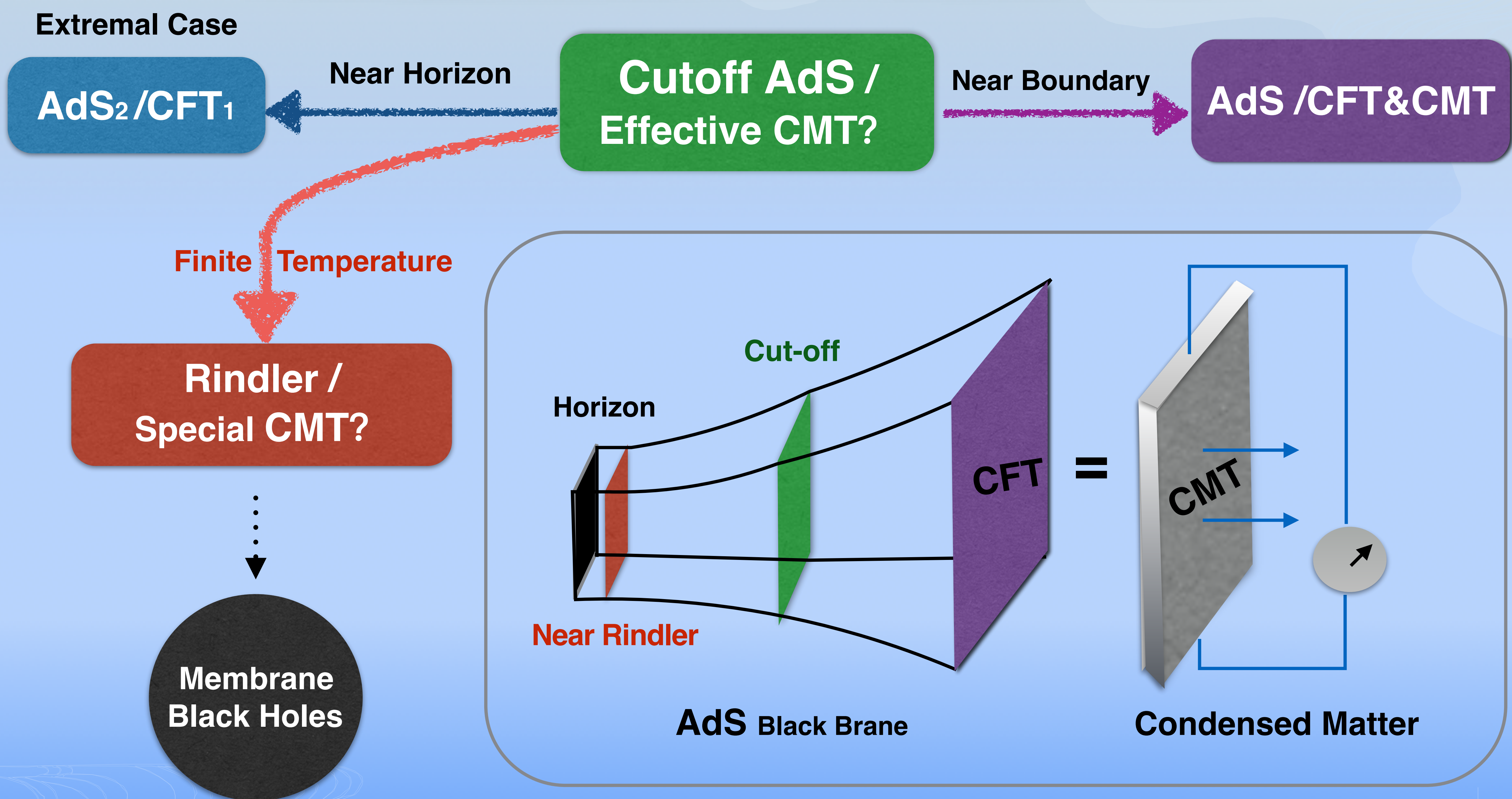

Motivations & Phase Diagrams

High Tc superconductors

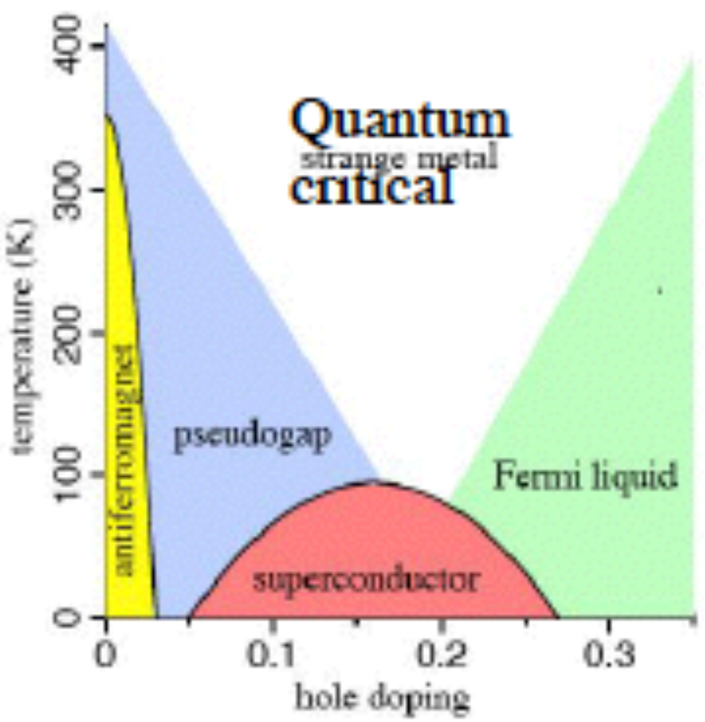

Heavy fermions

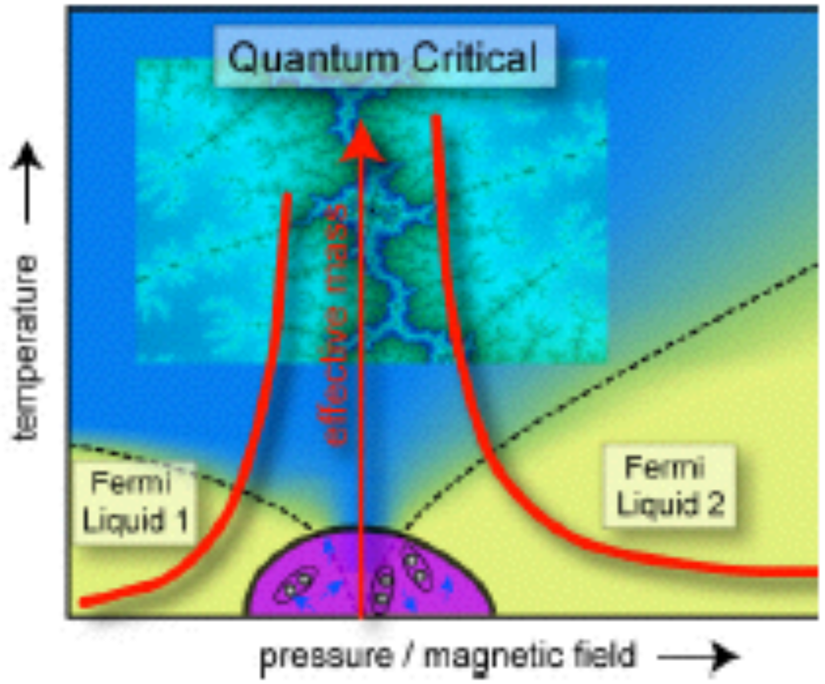

Iron superconductors (?)

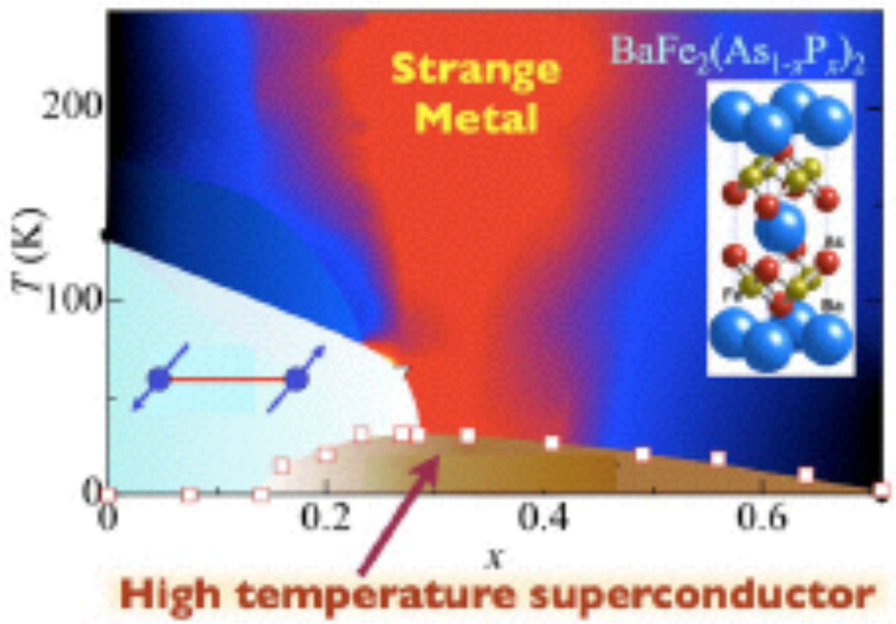

Figures credit: J. Zaanen

1. Holographic Properties of Black Hole

(Relevant topics)

(2010s) Emergent Gravity:	Information Metric
(2000s) AdS/CFT Duality:	Black Hole in a Box
(1990s) Holographic Principle:	Horizon Encoding
(1980s) Membrane Paradigm:	Effective Fluid
(1970s) Hawking Radiation:	Thermodynamics

Historical Models of Black Hole (~1960s)

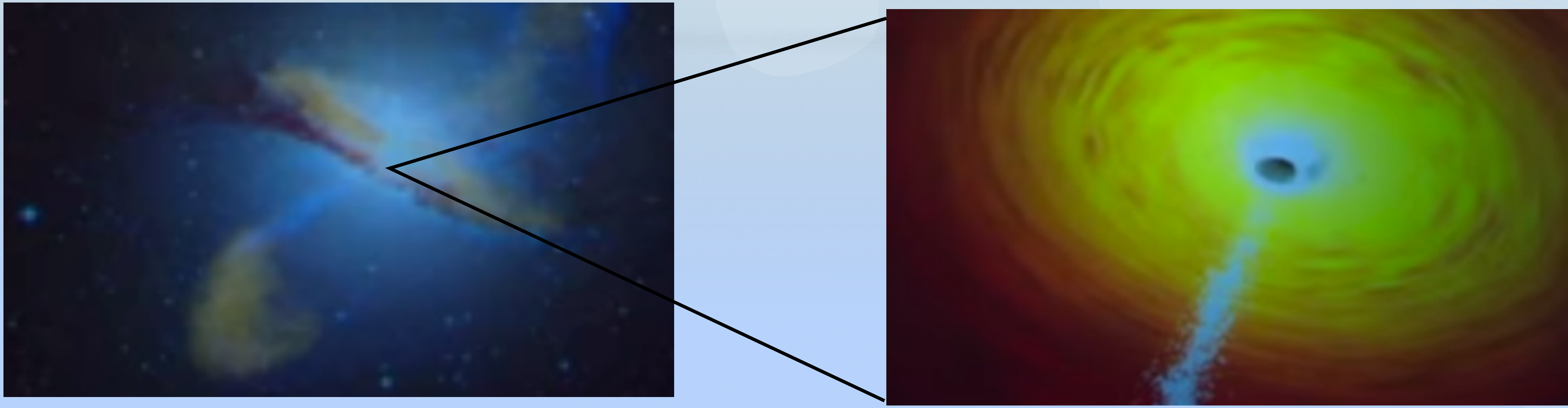

Dark Stars: Newton's Gravity (1687)

Frozen Stars: Einstein's Gravity (1915)

Schwarzschild Solution(1916)

$$c^2 d\tau^2 = \left(1 - \frac{r_s}{r}\right) c^2 dt^2 - \left(1 - \frac{r_s}{r}\right)^{-1} dr^2 - r^2 \left(d\theta^2 + \sin^2\theta \, d\varphi^2\right),$$

Black Holes: Golden age of general relativity(1960s):

Kerr-Newman Solution

Figures credit: World Science Festival

Thermodynamics (1970s): Hawking Radiation

Bekenstein & Hawking, …

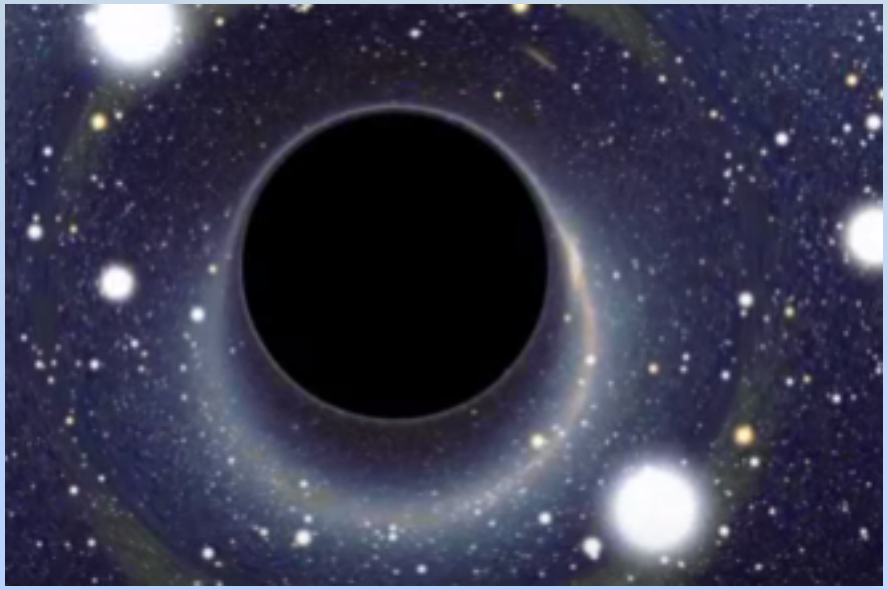

Hawking Temperature $T_H = \frac{\hbar c^3}{8\pi G M k_B} = \frac{\kappa}{2\pi},$

Bekenstein-Hawking Entropy $S_{\mathrm{BH}} = \frac{kA}{4\ell_{\mathrm{P}}^2}$

0th Law: constant surface gravity

1st Law: $dE = \frac{\kappa}{8\pi} dA + \Omega\, dJ + \Phi\, dQ,$

2nd Law: non-decreasing of entropy

3rd Law: extremal black hole is not possible

Membrane paradigm(1980s): Effective Fluid

Doumer & Thorne, …

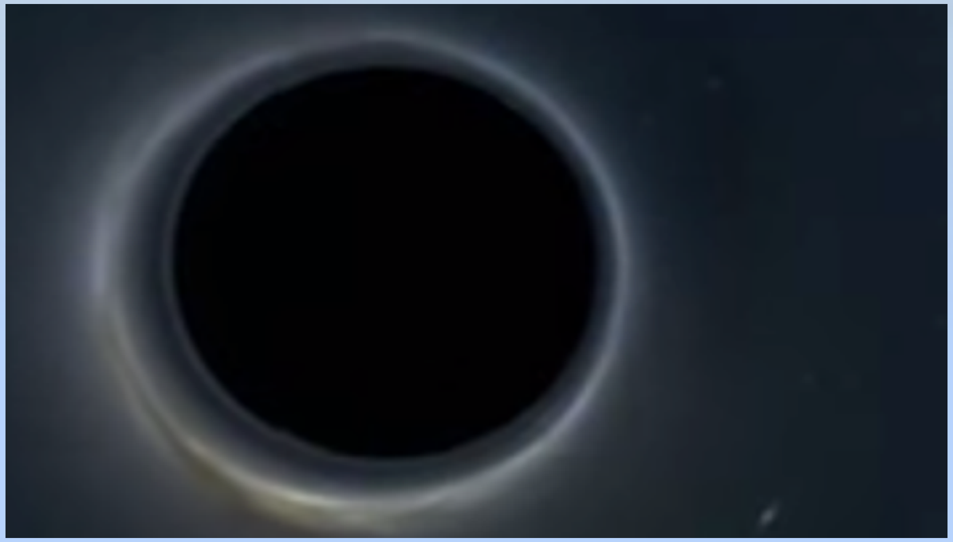

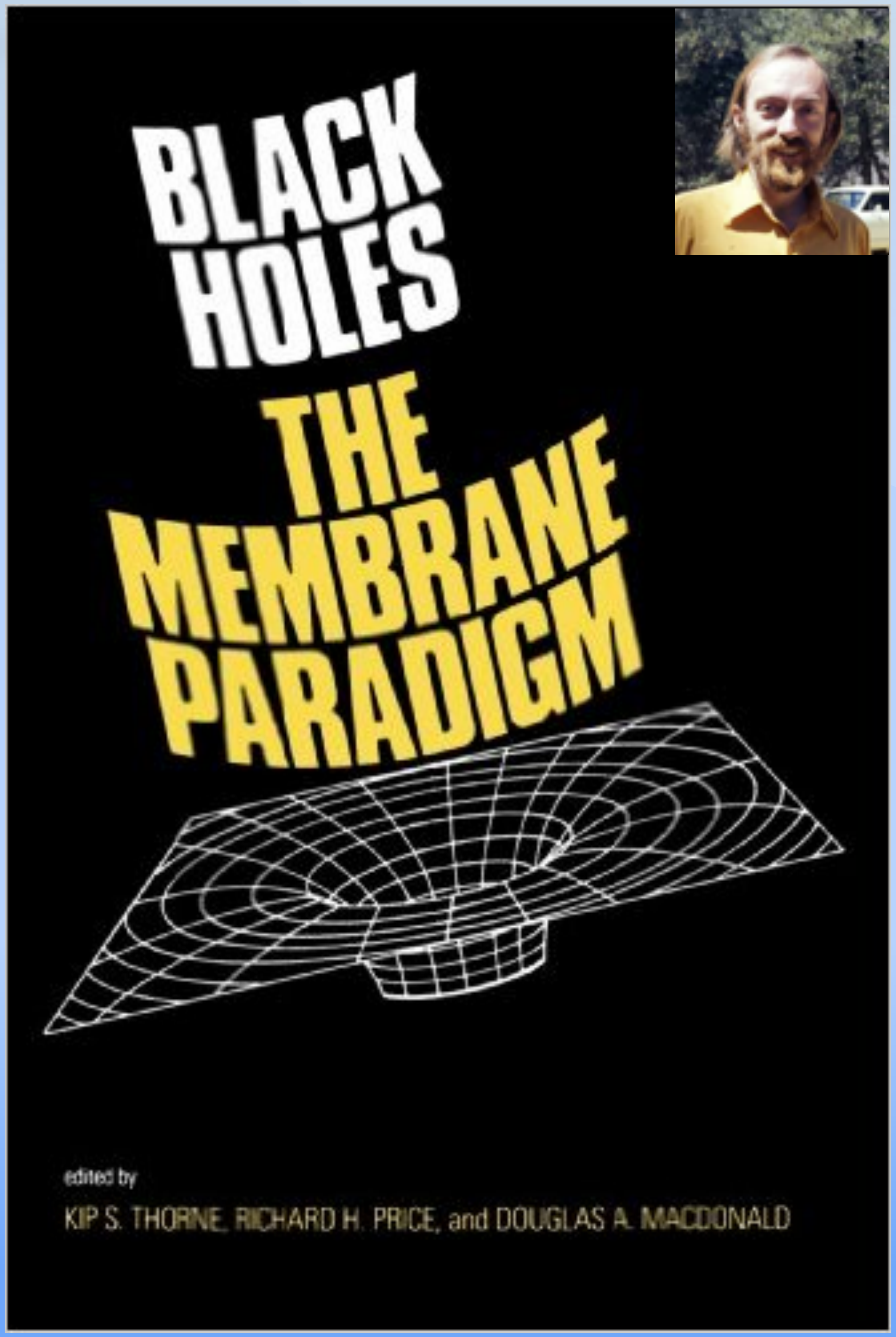

Effective Description

Stretched horizon

Conductivity & Viscosity

Holographic Principle (1990s): Horizon encoding

Susskind & ’t Hooft, …

Black hole Horizon

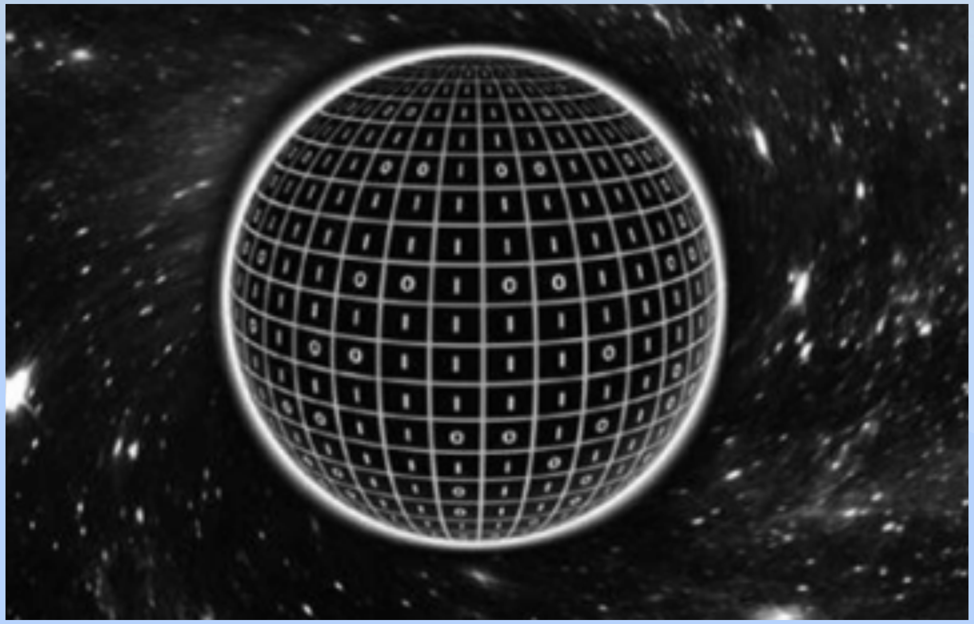

Gravity in the Bulk=
Theory on the light-like boundary

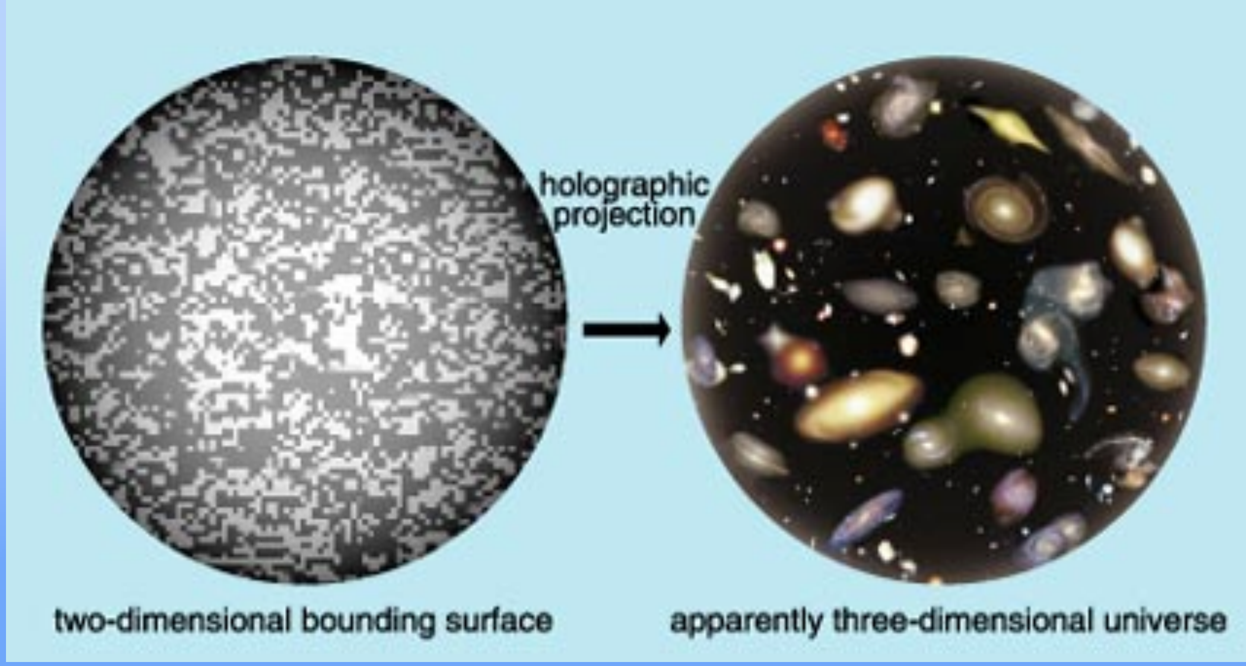

Cosmological Horizon

AdS/CFT Duality (2000s):

Maldacena & Gubser & Witten, …

AdS/CMT: D.Son & S. Hartnoll & H. Liu…

Black Hole in a natural Box

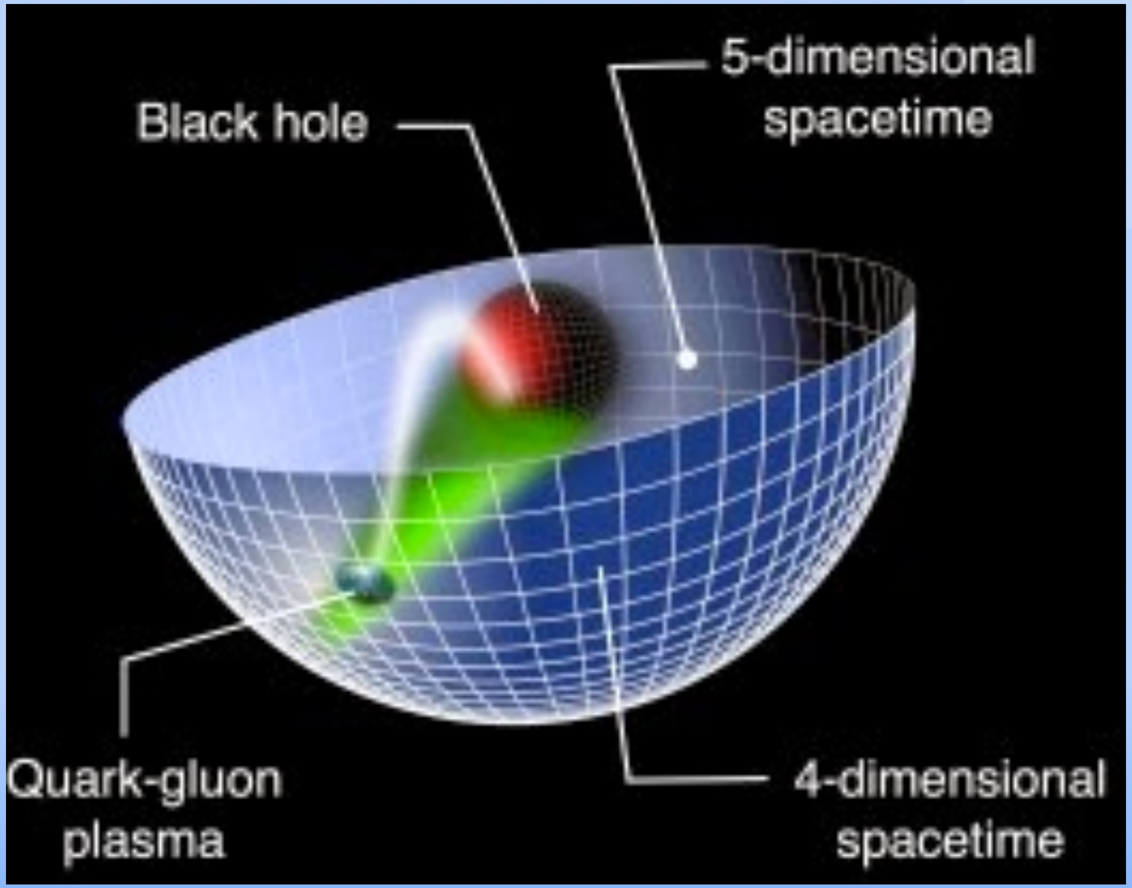

Conductivity

Shear Viscosity $\frac{\eta}{s} \approx \frac{\hbar}{4\pi k}$

Holographic Superconductor

Holographic Non-Fermi Liquid

Emergent Gravity (2010s)

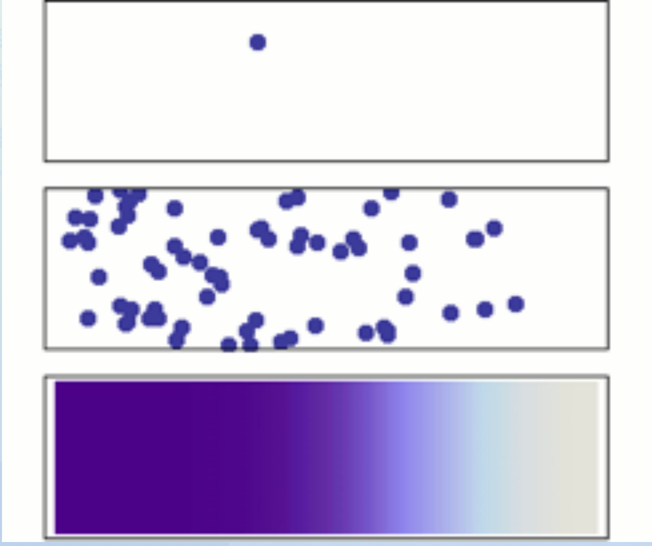

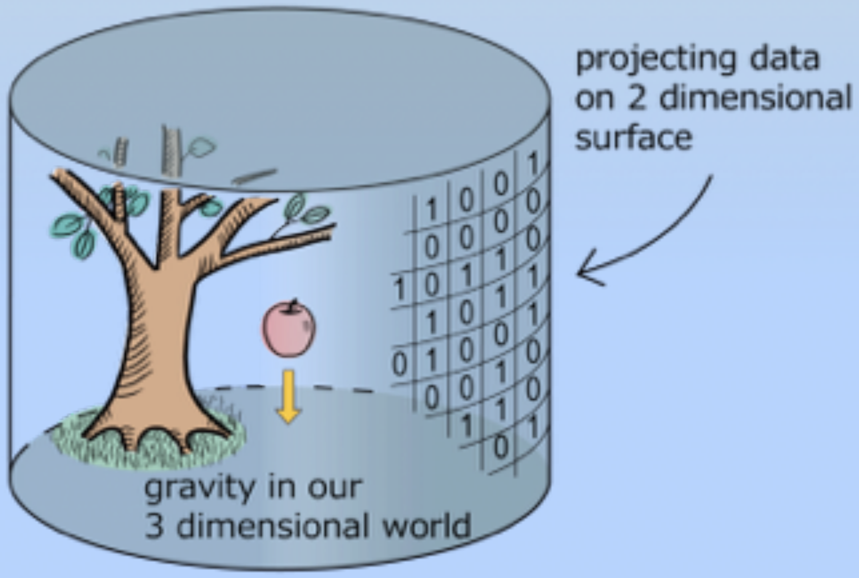

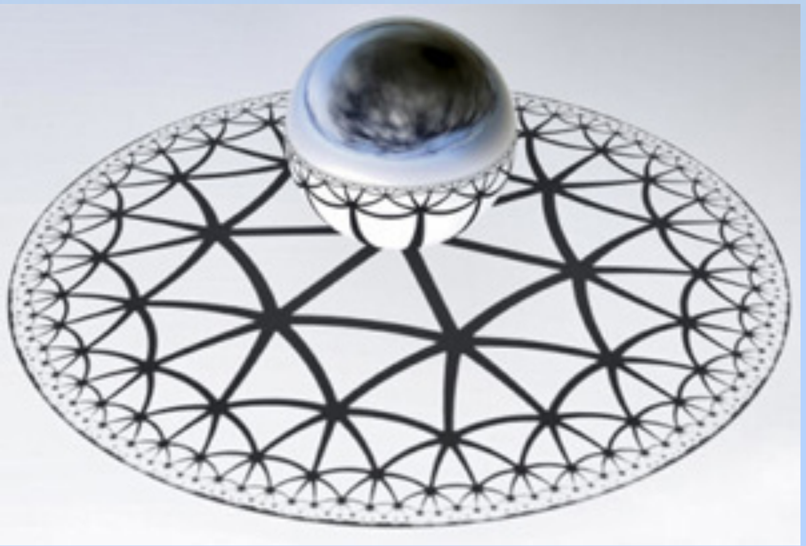

Emergent Gravity from Entropic Force (E. Verlinde)

Holographic Geometry from Tensor Network (S.Ryu &T. Takayanagi)

Emergent Spacetime from Quantum Entanglement (H. Ooguri)

2. Engineering Holographic Phase Diagrams with Dome

$$\mathcal{L}_M = \sum_{i=1,2} \mathcal{L}_{\psi_i} + \mathcal{L}_\phi + \mathcal{L}_{int}, \qquad g_M^2 \mathcal{L}_{int} = -\frac{1}{2}\sum_{i=1,2} F_i(\phi)\psi_i^2,$$

$$g_M^2 \mathcal{L}_{\psi_i} = -\frac{1}{2}(\partial\psi_i)^2 - V(\psi_i), \quad V(\psi_i) = \frac{1}{2}m_i^2\psi_i^2 + \frac{1}{4}\lambda_i\psi_i^4,$$

$$g_M^2 \mathcal{L}_\phi = -\frac{1}{2}(\partial\phi)^2 - V(\phi), \qquad V(\phi) = \frac{1}{2}m_\phi^2\phi^2 + \frac{1}{4}\lambda_\phi\phi^4,$$

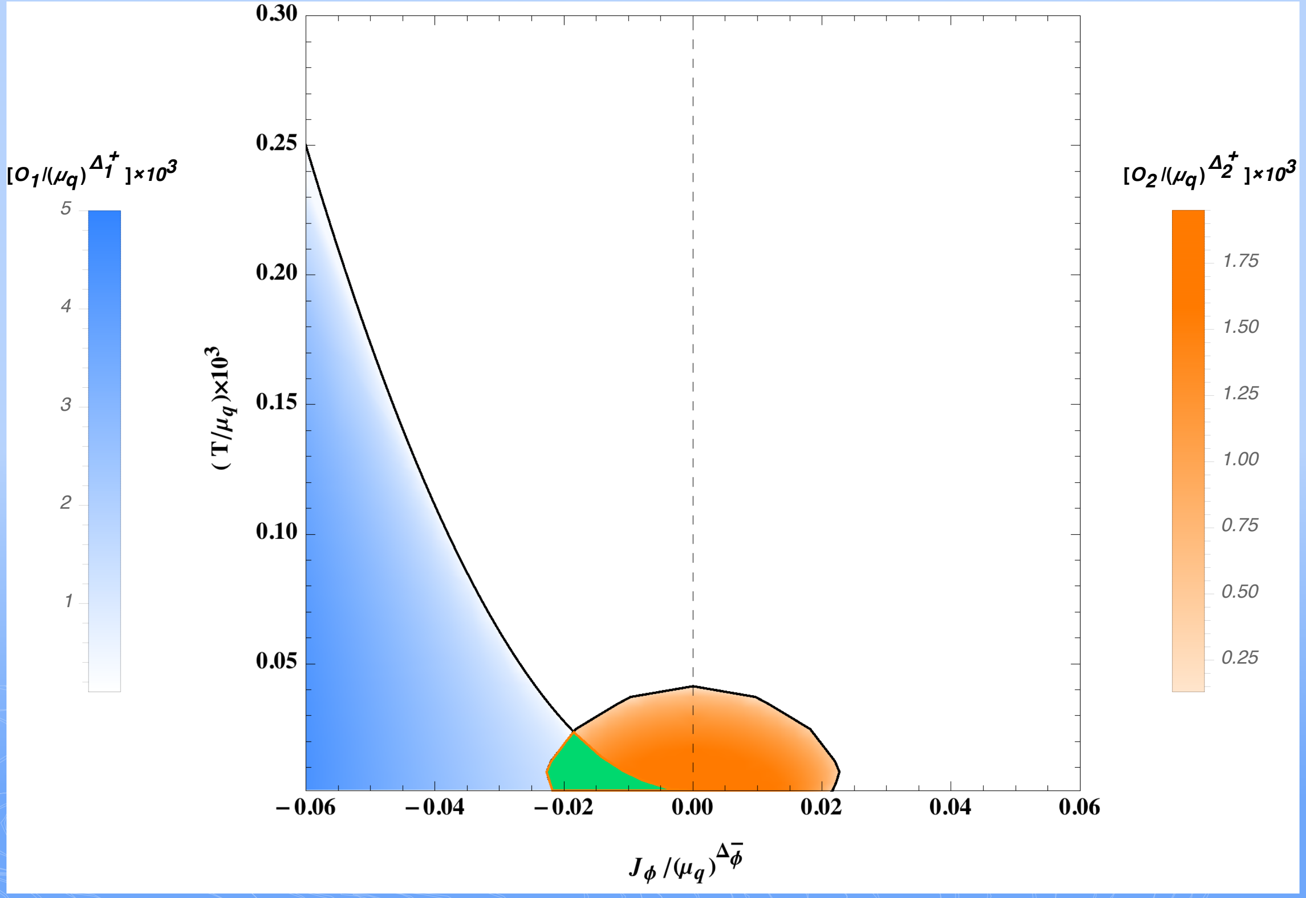

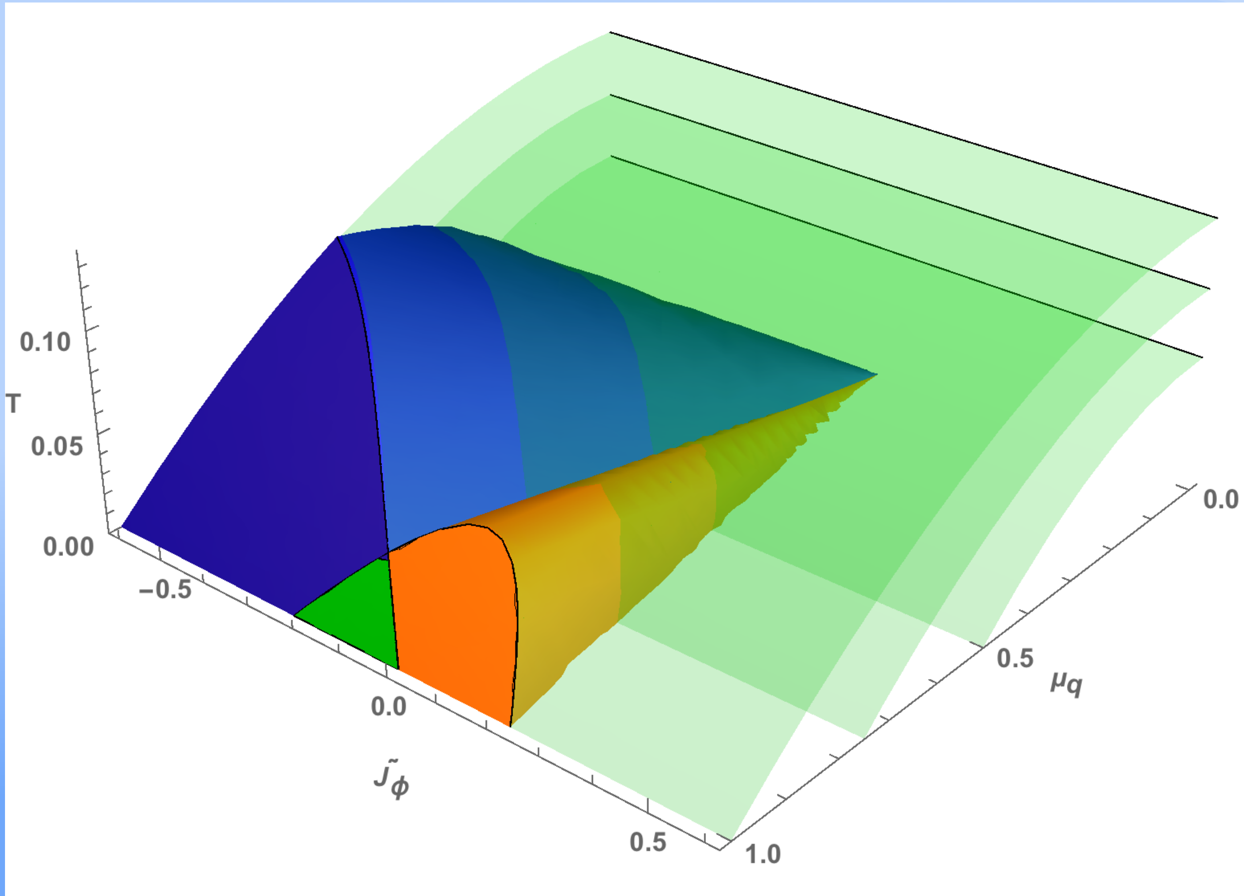

arXiv: 1603.08259 Jiunn-Wei Chen, Shou-Huang Dai, Debaprasad Maity, Yun-Long Zhang

Quantum critical region

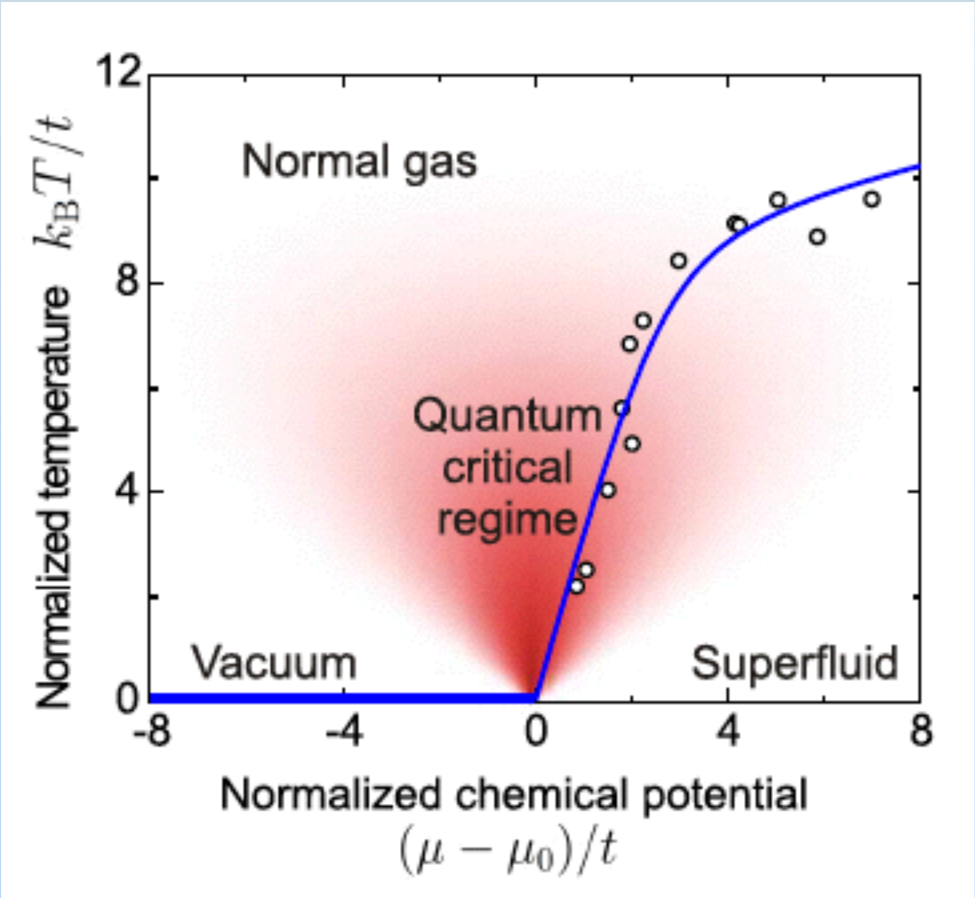

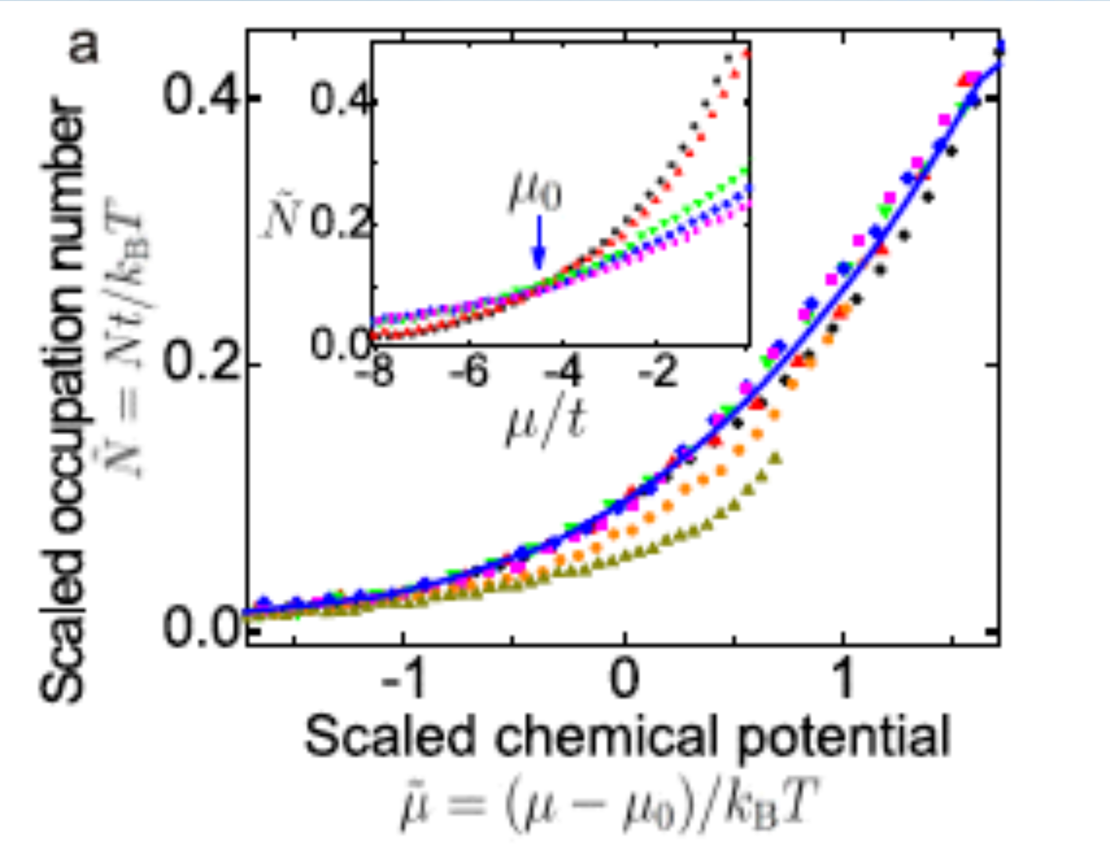

$$\frac{k_B T_c}{t} = c\left(\frac{\mu - \mu_0}{t}\right)^{z\nu},$$

$$\tilde{N} = F(\tilde{\mu}),$$

$$\tilde{N} = \frac{N - N_r}{(\frac{k_B T}{t})^{\frac{D}{z}+1-\frac{1}{z\nu}}} \text{ and } \tilde{\mu} = \frac{\frac{\mu - \mu_0}{t}}{(\frac{k_B T}{t})^{\frac{1}{z\nu}}}$$

Science 335, 6072 (2012). Quantum critical behavior of ultracold atoms in two-dimensional optical lattices

Background Gravity

$$S_{bulk} = \int \mathrm{d}^4x\sqrt{-g}\left[\frac{1}{2\kappa^2}(R-2\Lambda) - \frac{L^2}{2\kappa^2}\frac{1}{g_F^2}F^2\right] + S_{b.t.} + \int \mathrm{d}^4x\sqrt{-g}\,(\mathcal{L}_M) + S_{c.t.},$$

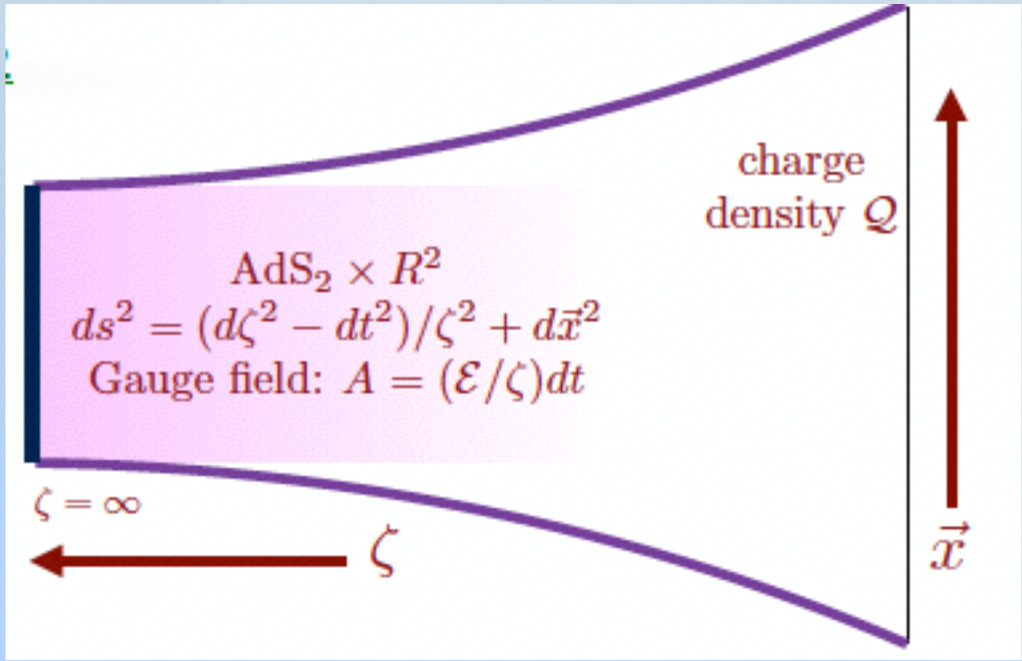

$$ds^2 = \frac{r^2}{L^2}\left[-f(r)dt^2 + dx^2 + dy^2\right] + \frac{L^2}{r^2}\frac{dr^2}{f(r)},$$

$$F = g_F \frac{q}{L^2}\frac{r_h^2}{r^2}\mathrm{d}r \wedge \mathrm{d}t,$$

$$T = \frac{3}{4\pi}\frac{r_h}{L^2}\left[1 - \frac{q^2}{3}\right], \qquad s = \frac{2\pi}{\kappa^2}\frac{r_h^2}{L^2}.$$

$$\mu_q = g_F q \frac{r_h}{L^2}, \qquad n_q = \frac{2q}{\kappa^2 g_F}\frac{r_h^2}{L^2}.$$

$$f(r) = 1 - (1+q^2)\frac{r_h^3}{r^3} + q^2\frac{r_h^2}{r^4},$$

$$A_t(r) = g_F \frac{q\, r_h}{L^2}\left(1 - \frac{r_h}{r}\right).$$

$$n_q(\mu_q, T) = \frac{4\pi}{3\kappa^2}\frac{L^2}{g_F^2}\mu_q T\left(1 + \sqrt{1 + \frac{3}{4\pi^2 g_F^2}\frac{\mu_q^2}{T^2}}\right)$$

H. Liu, S. Sachdev , et al.

Scaling symmetries

$$r \to \lambda r, \quad \{t, x, y\} \to \lambda^{-1}\{t, x, y\},$$

$$\{r_h, T, \mu_q\} \to \lambda\{r_h, T, \mu_q\}, \qquad \{s, n_q\} \to \lambda^2\{s, n_q\}.$$

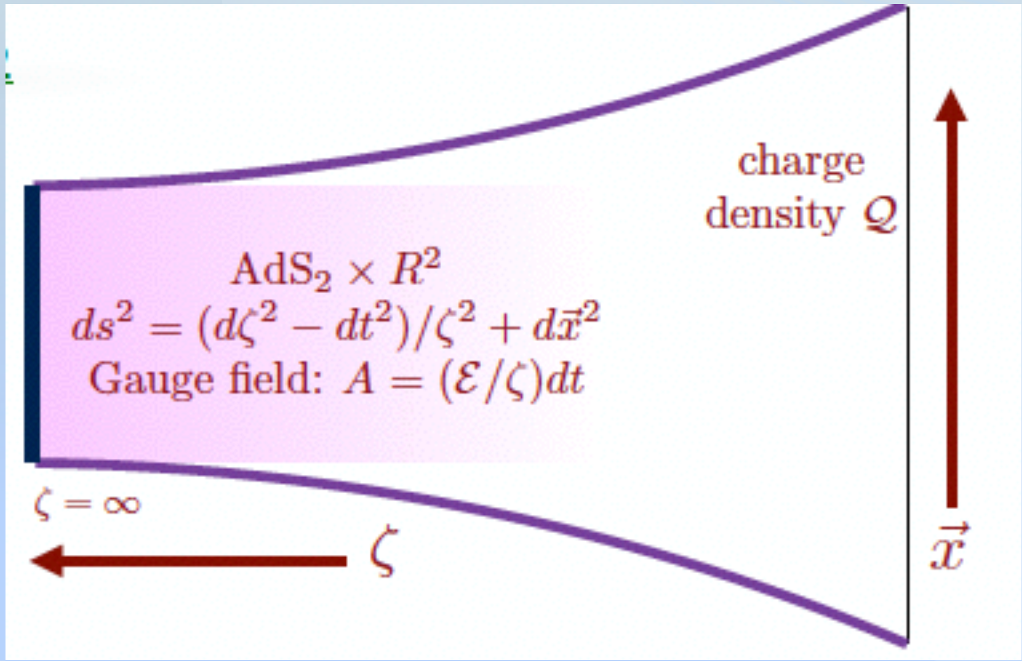

$$\tilde{n}_q(\tilde{\mu}_q) = \frac{4\pi}{3}\tilde{\mu}_q\left(1 + \sqrt{1 + \frac{3}{4\pi^2}\tilde{\mu}_q^2}\right).$$

$$\tilde{n}_q = (n_q g_F \kappa^2)/(T^2 L^2)$$

$$n_q(\mu_q, T) = \frac{4\pi}{3\kappa^2}\frac{L^2}{g_F^2}\mu_q T\left(1 + \sqrt{1 + \frac{3}{4\pi^2 g_F^2}\frac{\mu_q^2}{T^2}}\right)$$

$$\tilde{\mu}_q = \mu_q/(T g_F)$$

H. Liu, S. Sachdev , et al.

BF bound in AdS

$$\mathcal{L}_\chi = \frac{1}{2\kappa^2\lambda}\left[-\frac{1}{2}(\partial\chi)^2 - V(\chi)\right]$$

$$V(\chi) = \frac{1}{4R^2}\left(\chi^2 + m^2R^2\right)^2 - \frac{m^4R^2}{4} \,.$$

$$-\frac{9}{4} < m^2R^2 < -\frac{3}{2} \,.$$

$$-\frac{d^2}{4} < m^2R^2 < -\frac{d(d-1)}{4} \,.$$

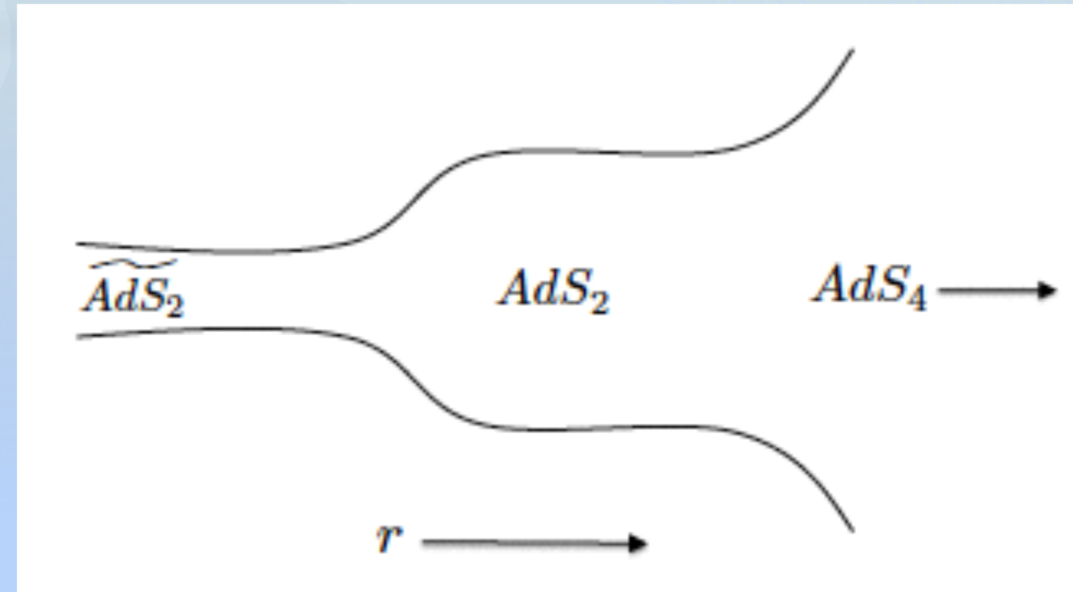

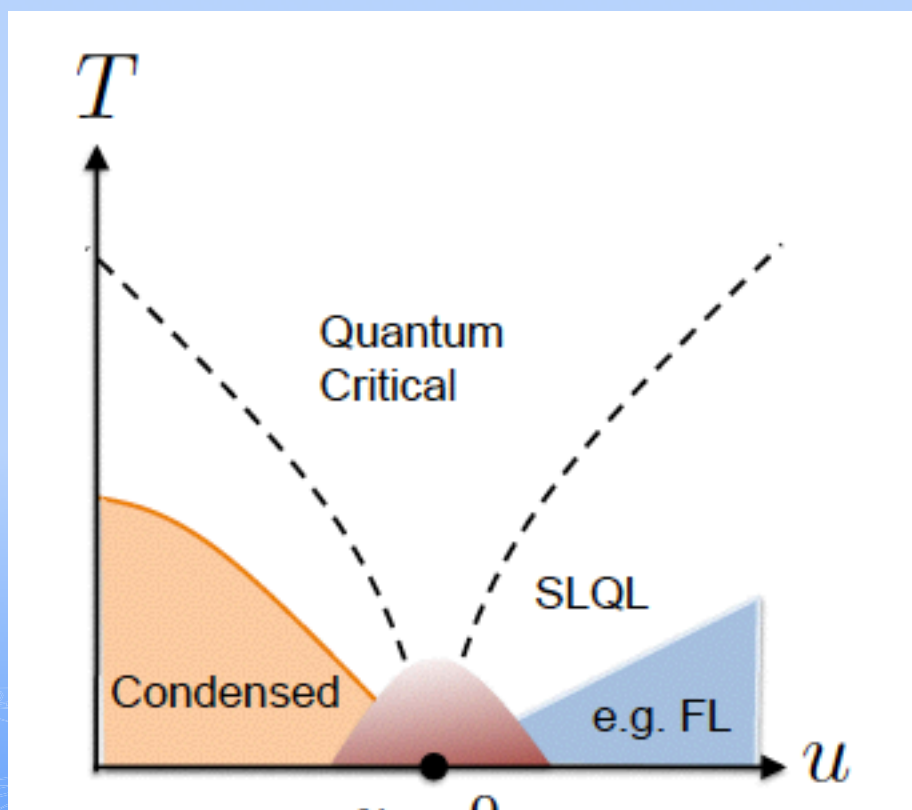

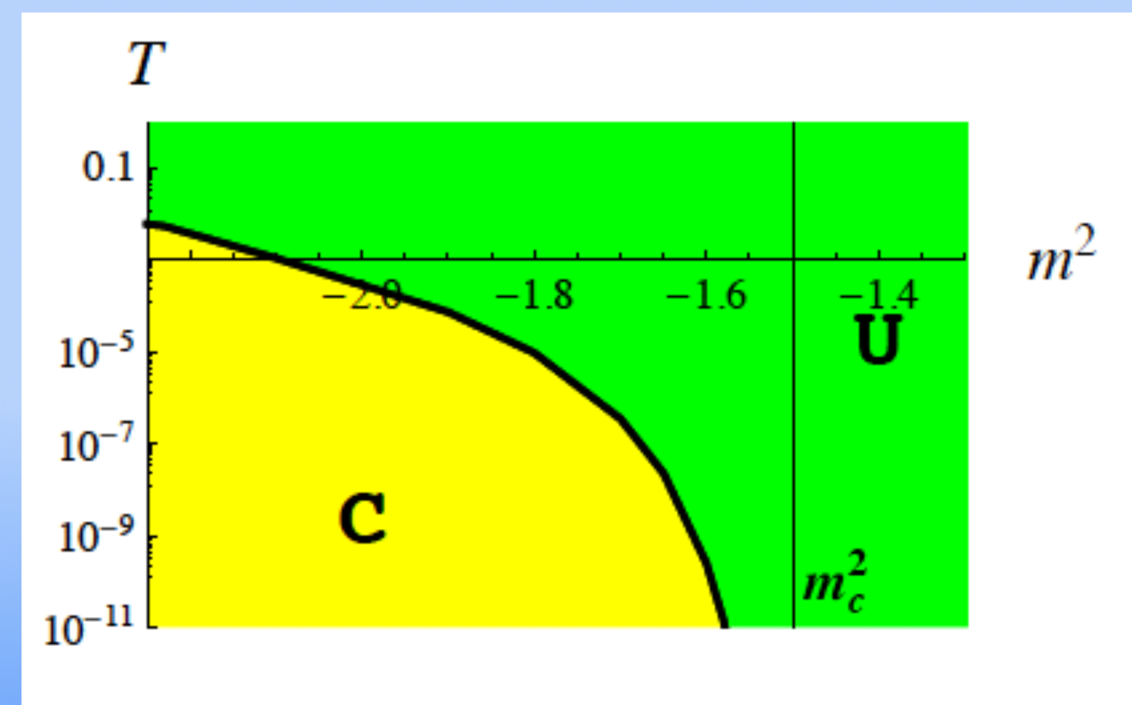

N. Iqbal, H. Liu, M. Mezei and Q. Si, 1003.0010

Single charged scalar field

$$g_M^2 \mathcal{L}_M = g_M^2 \mathcal{L}_\Psi = -\frac{1}{2}|\partial\Psi - i q_\Psi A \Psi|^2 - V(\Psi),$$
$$V(\Psi) = \frac{1}{2} m_\Psi^2 |\Psi|^2 + \frac{1}{4}\lambda_\Psi |\Psi|^4.$$

$$ds^2 = \frac{r^2}{L^2}\left[-f(r)dt^2 + dx^2 + dy^2\right] + \frac{L^2}{r^2}\frac{dr^2}{f(r)},$$
$$F = g_F \frac{q}{L^2}\frac{r_h^2}{r^2} \mathrm{d}r \wedge \mathrm{d}t,$$

$$\frac{1}{r^2 L^2}\partial_r\left[r^4 f(r)\partial_r \Psi\right] - \left(m_\Psi^2 - \frac{L^2 q_\Psi^2 A_t(r)^2}{r^2 f(r)}\right)\Psi - \lambda_\Psi |\Psi|^2 \Psi = 0.$$

$$\Psi \to \frac{J_\Psi}{r^{\Delta_\Psi^-}} + \frac{O_\Psi}{r^{\Delta_\Psi^+}} + \dots,$$

$$J_\Psi \to \lambda^{\Delta_\Psi^-} J_\Psi, \qquad O_\Psi \to \lambda^{\Delta_\Psi^+} O_\Psi.$$

$$\Delta_\Psi^\pm = \frac{3}{2} \pm \sqrt{\frac{9}{4} + m_\Psi^2 L^2},$$

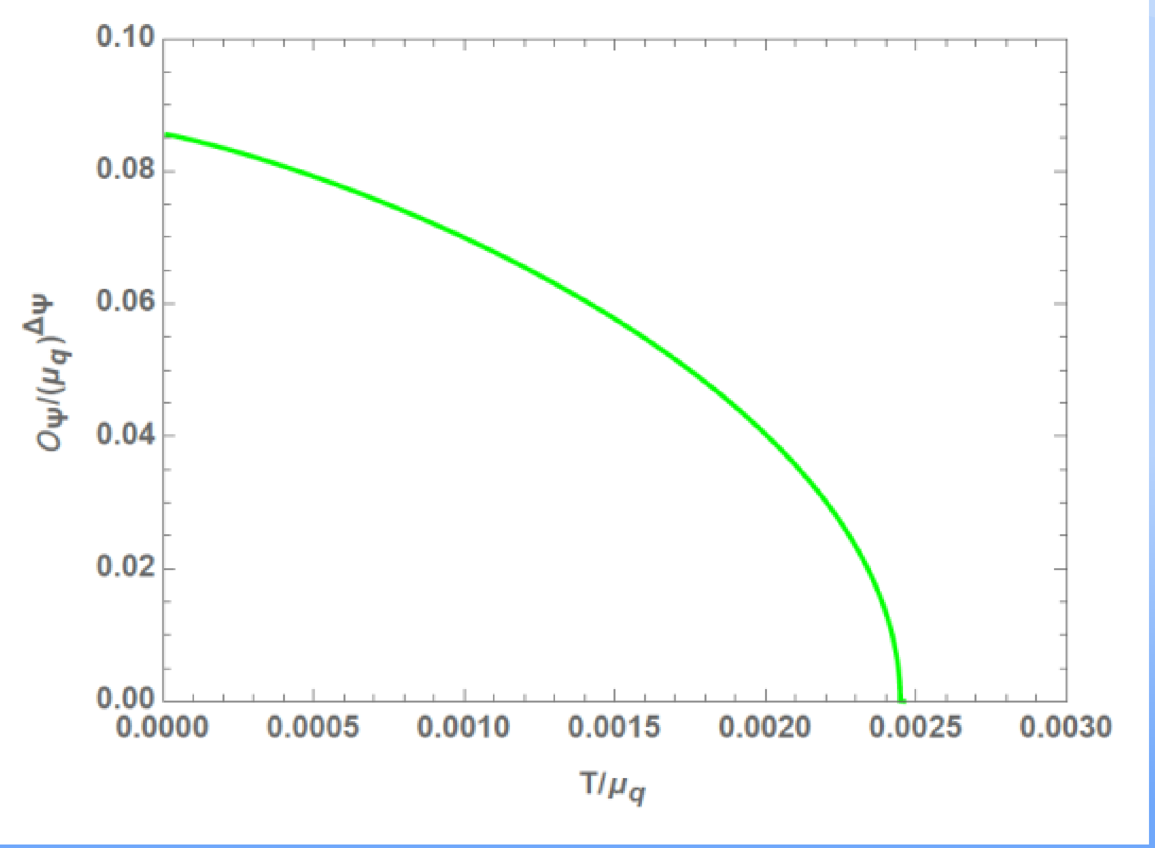

A minimal Model

$$\mathcal{L}_M = \sum_{i=1,2} \mathcal{L}_{\psi_i} + \mathcal{L}_\phi + \mathcal{L}_{int},$$

$$g_M^2 \mathcal{L}_{\psi_i} = -\frac{1}{2}(\partial\psi_i)^2 - V(\psi_i), \quad V(\psi_i) = \frac{1}{2}m_i^2\psi_i^2 + \frac{1}{4}\lambda_i\psi_i^4,$$

$$g_M^2 \mathcal{L}_\phi = -\frac{1}{2}(\partial\phi)^2 - V(\phi), \quad V(\phi) = \frac{1}{2}m_\phi^2\phi^2 + \frac{1}{4}\lambda_\phi\phi^4,$$

$$\psi_i(r) \to \frac{J_i}{r^{\Delta_i^-}} + \frac{O_i}{r^{\Delta_i^+}}, \qquad \Delta_i^\pm = \frac{3}{2} \pm \sqrt{\frac{9}{4} + m_i^2},$$

$$\phi(r) \to \frac{J_\phi}{r^{\Delta_\phi^-}} + \frac{O_\phi}{r^{\Delta_\phi^+}}, \qquad \Delta_\phi^\pm = \frac{3}{2} \pm \sqrt{\frac{9}{4} + m_\phi^2}.$$

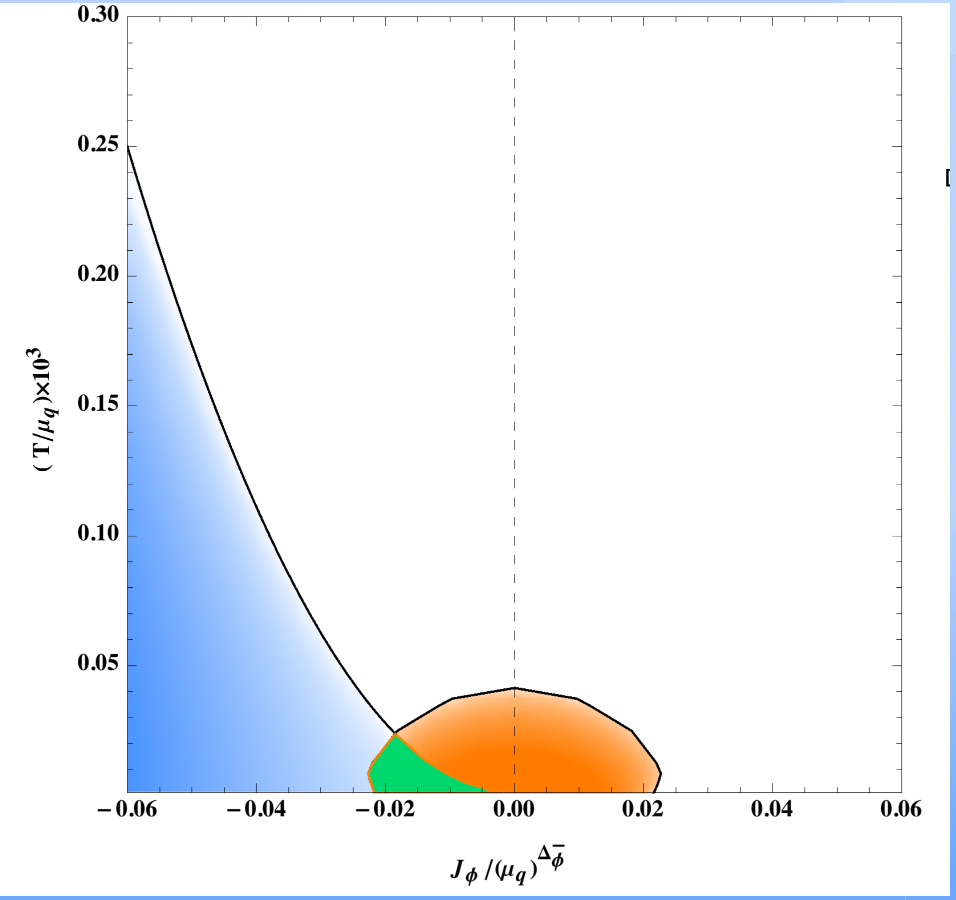

Effective internation

$$g_M^2 \mathcal{L}_{int} = -\frac{1}{2}\sum_{i=1,2} F_i(\phi)\psi_i^2,$$

Model I: Parameters with Positive Doping

Phase diagram with $-F_2(\phi) = \phi^2 - \frac{5}{24}\phi^4 \cong F_1(\phi).$

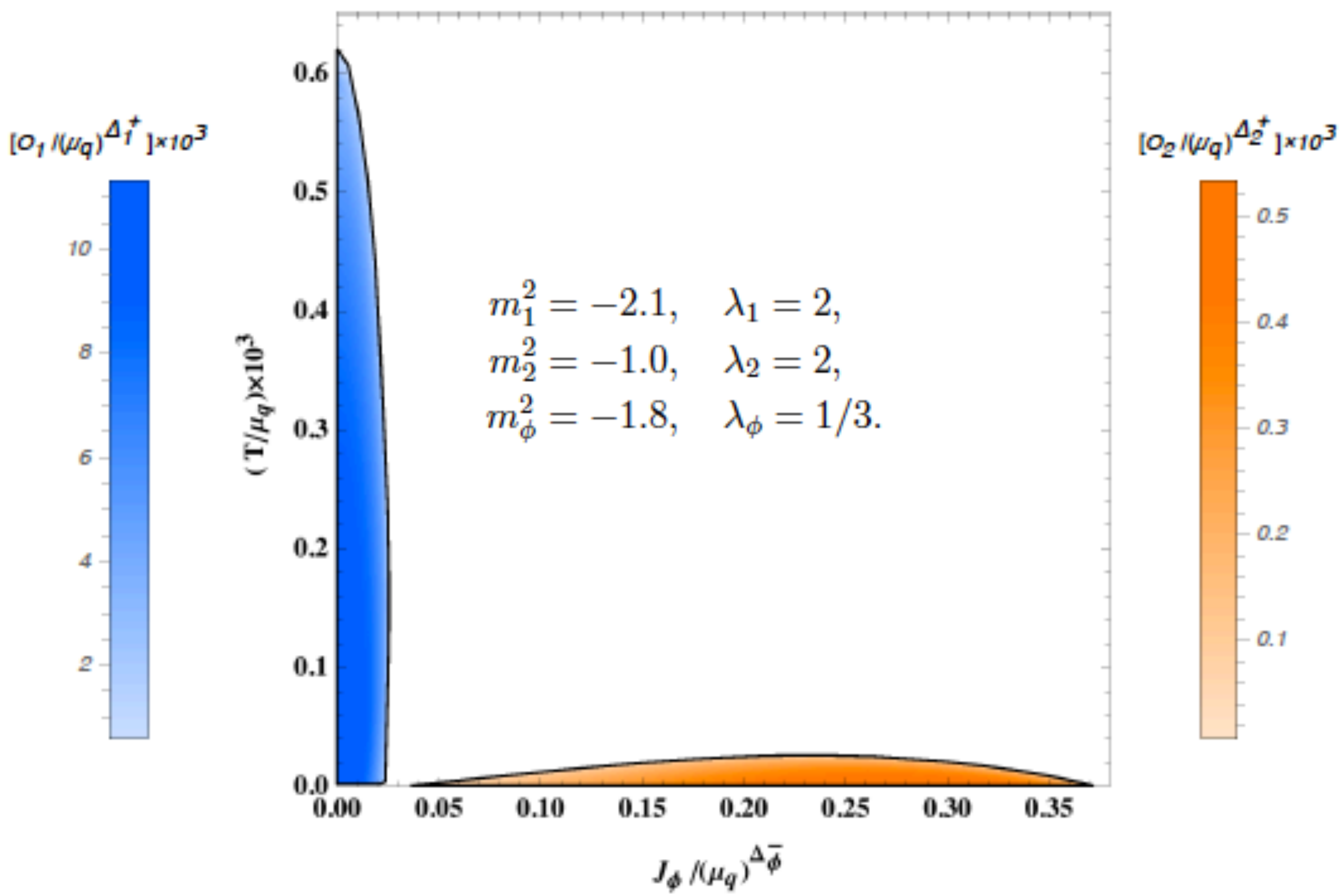

Figure 2: The phase diagram of model I with positive dopping parameter. It is the density plot for phase 1(blue) and phase 2 (orange) with coupling functions $-F_2(\phi) = \phi^2 - 5\phi^4/24 \cong F_1(\phi)$.

Model I: Free Energy difference

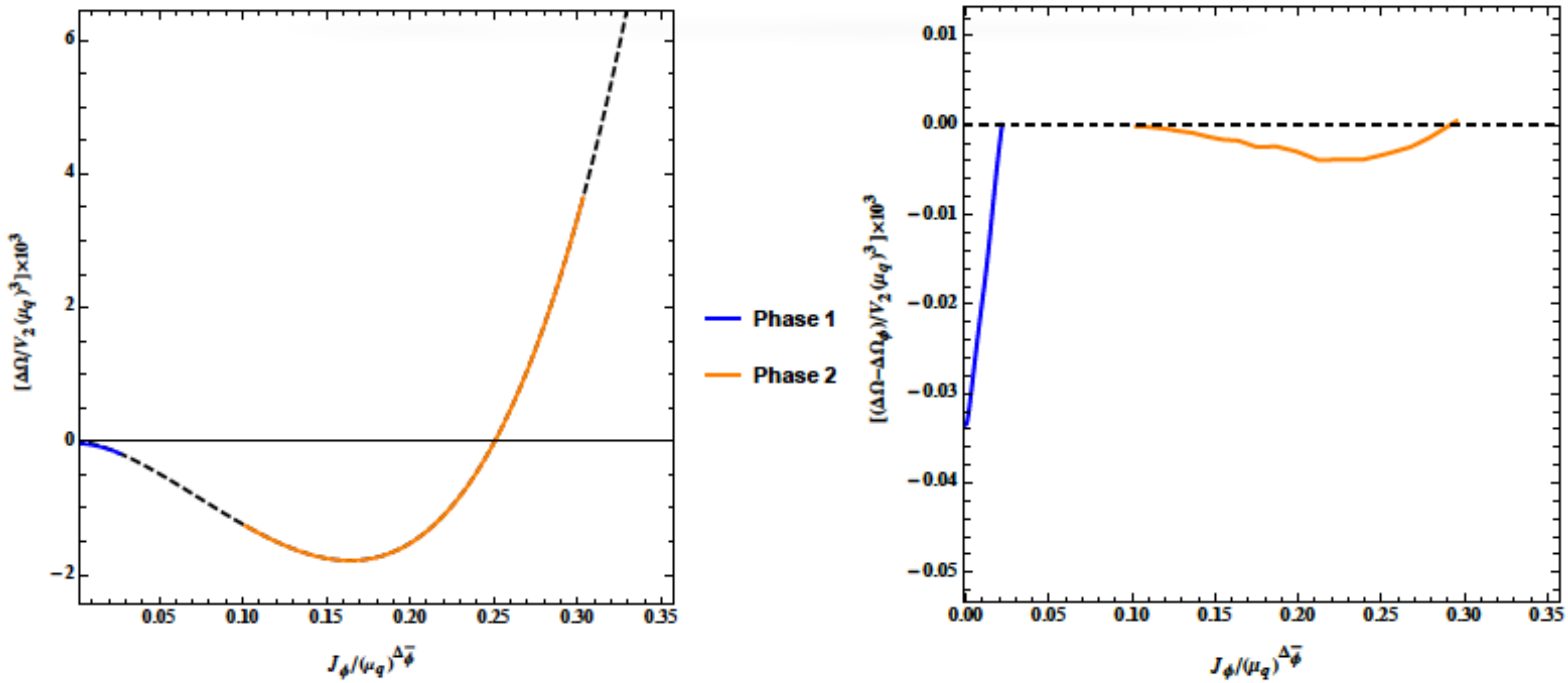

Figure 6: Left, the free energy density in Figure 5 at $(T/\mu_q) \times 10^3 \simeq 0.014$. The dashed black line indicate the normal phase with only one turning field ϕ. The Blue and Orange line corresponding to Phase 1 and Phase 2, respectively. Right, the energy difference between the ordered and normal phase

Model II: Dome around Critical Point

Phase diagram with $F_1(\phi) = \phi(\phi + 2)$ $F_2(\phi) = \phi^2/2$

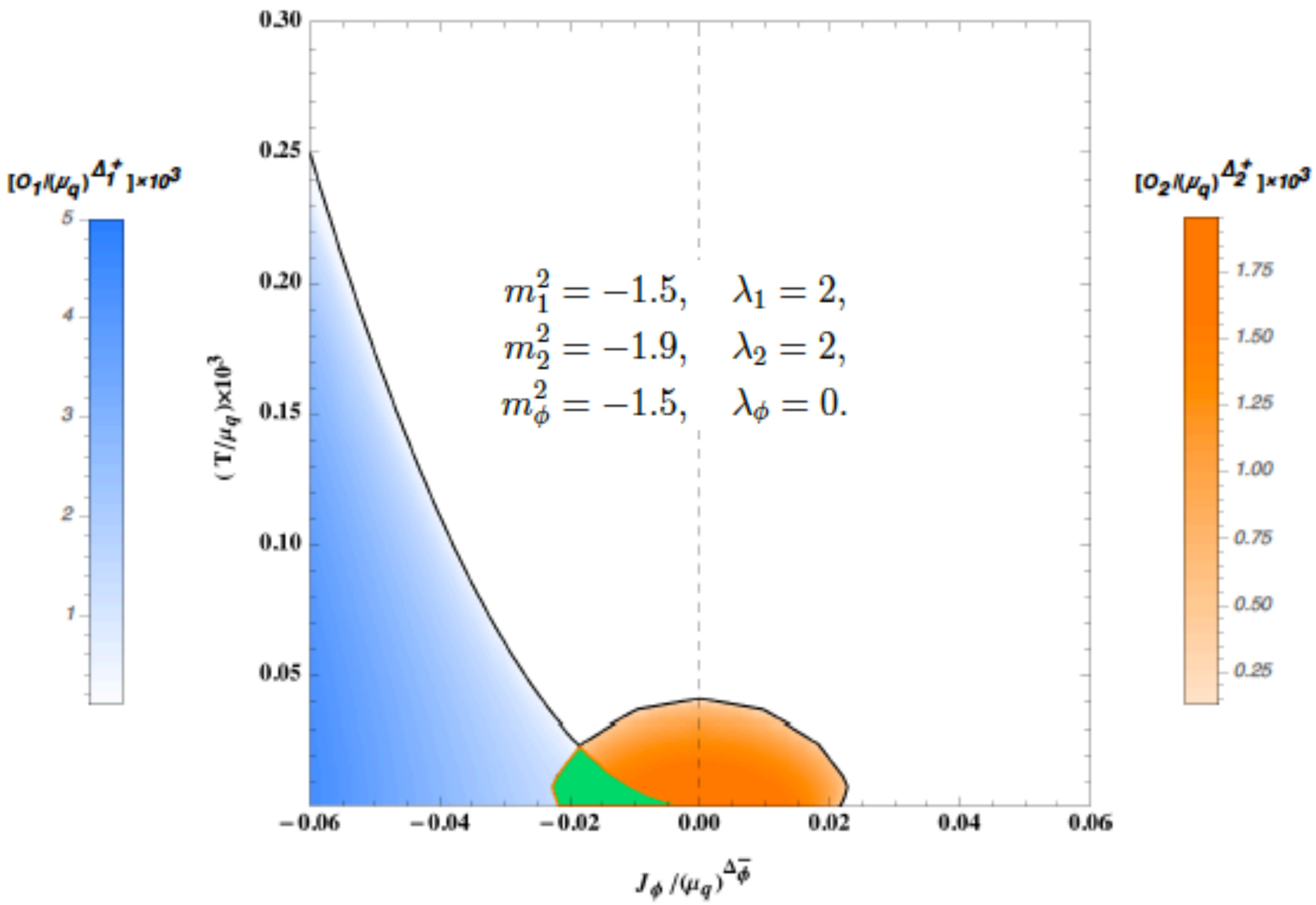

Figure 4: The phase diagram of model II around a natural quantum critical point. It is the density plot phase 1(blue) and phase 2 (orange) with coupling functions $F_1(\phi) = \phi(\phi + 2)$, $F_2(\phi) = \phi^2/2$. The green parts are the overlap region.

Model II: Free energy difference

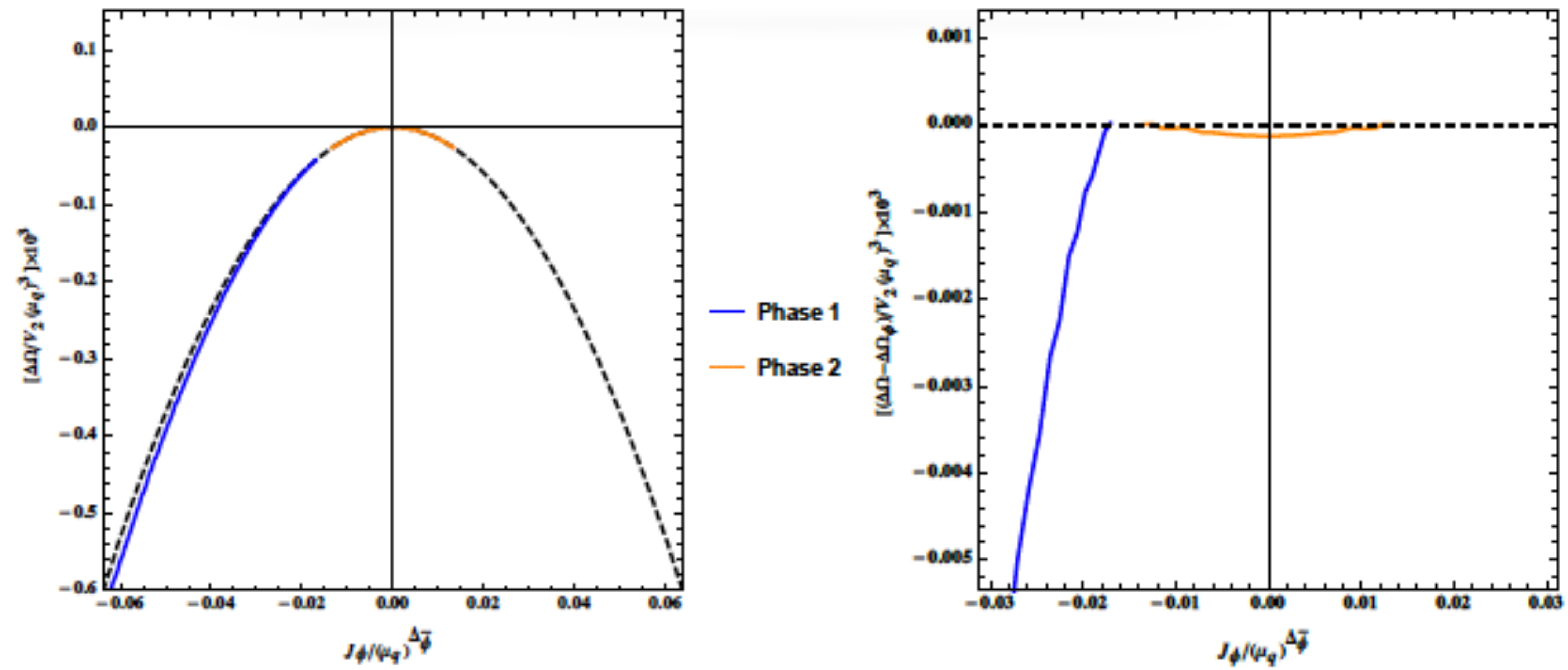

Figure 3: Left: The free energy density in Figure 2 at $(T/\mu_q)\times10^3 \simeq 0.028$. The dashed black line indicate the normal phase with only one turning field ϕ. The blue and orange line corresponding to Phase 1 and Phase 2, respectively. Right, The energy difference between the ordered and normal phase

Relation with other models

$$S = \frac{1}{2\kappa_N^2}\int d^4x\sqrt{-g}\,[\mathcal{R} - 2\Lambda + \mathcal{L}_m + \mathcal{L}_{cs}]\,, \qquad (2.1)$$

$$\begin{aligned}\mathcal{L}_m = & -\frac{Z_G}{4}G^a_{\mu\nu}G^{a\mu\nu} - \frac{1}{2}D_\mu\Phi^a D^\mu\Phi^a - \frac{Z_A}{4}A_{\mu\nu}A^{\mu\nu} - \frac{Z_B}{4}B_{\mu\nu}B^{\mu\nu} - \frac{Z_{AB}}{2}A_{\mu\nu}B^{\mu\nu} \\ & -\frac{1}{2}\nabla_\mu\chi\nabla^\mu\chi - \mathcal{F}(\chi)(\nabla_\mu\theta - q_A A_\mu - q_B B_\mu)^2 - \frac{1}{2}\nabla_\mu\alpha\nabla^\mu\alpha - V_{int}, \qquad (2.2) \\ \mathcal{L}_{cs} = & -\vartheta_1(\alpha)\epsilon^{\mu\nu\lambda\sigma}A_{\mu\nu}A_{\lambda\sigma} - \vartheta_2(\alpha)\epsilon^{\mu\nu\lambda\sigma}A_{\mu\nu}B_{\lambda\sigma}.\end{aligned}$$

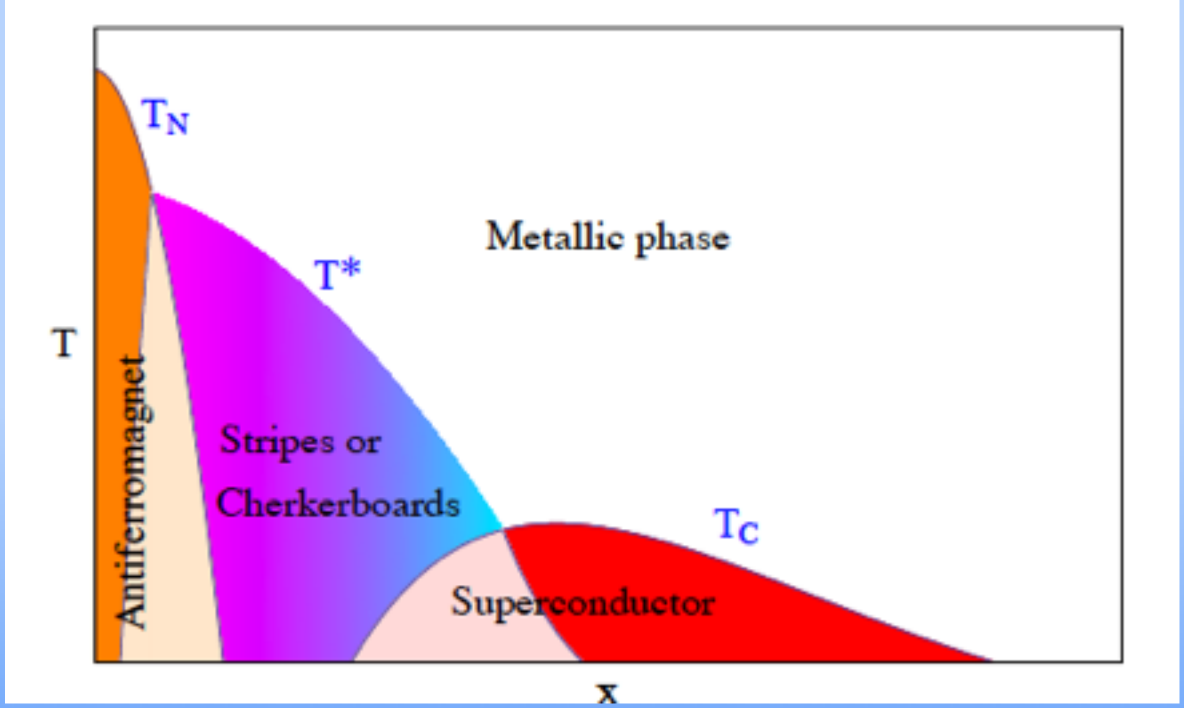

E. Kiritsis and L. Li, Holographic Competition of Phases and Superconductivity, JHEP 1601, 147 (2016)

3. Scaling symmetry in the models

$$\{r_h, T, \mu_q\} \to \lambda\{r_h, T, \mu_q\}, \qquad \{s, n_q\} \to \lambda^2\{s, n_q\}.$$

$$r \to \lambda r, \quad \{t, x, y\} \to \lambda^{-1}\{t, x, y\},$$

$$\{J_i, J_\phi\} \to \{\lambda^{\Delta_i^-} J_i,\ \lambda^{\Delta_\phi^-} J_\phi\}, \qquad \{O_i, O_\phi\} \to \{\lambda^{\Delta_i^+} O_i,\ \lambda^{\Delta_\phi^+} O_\phi\}.$$

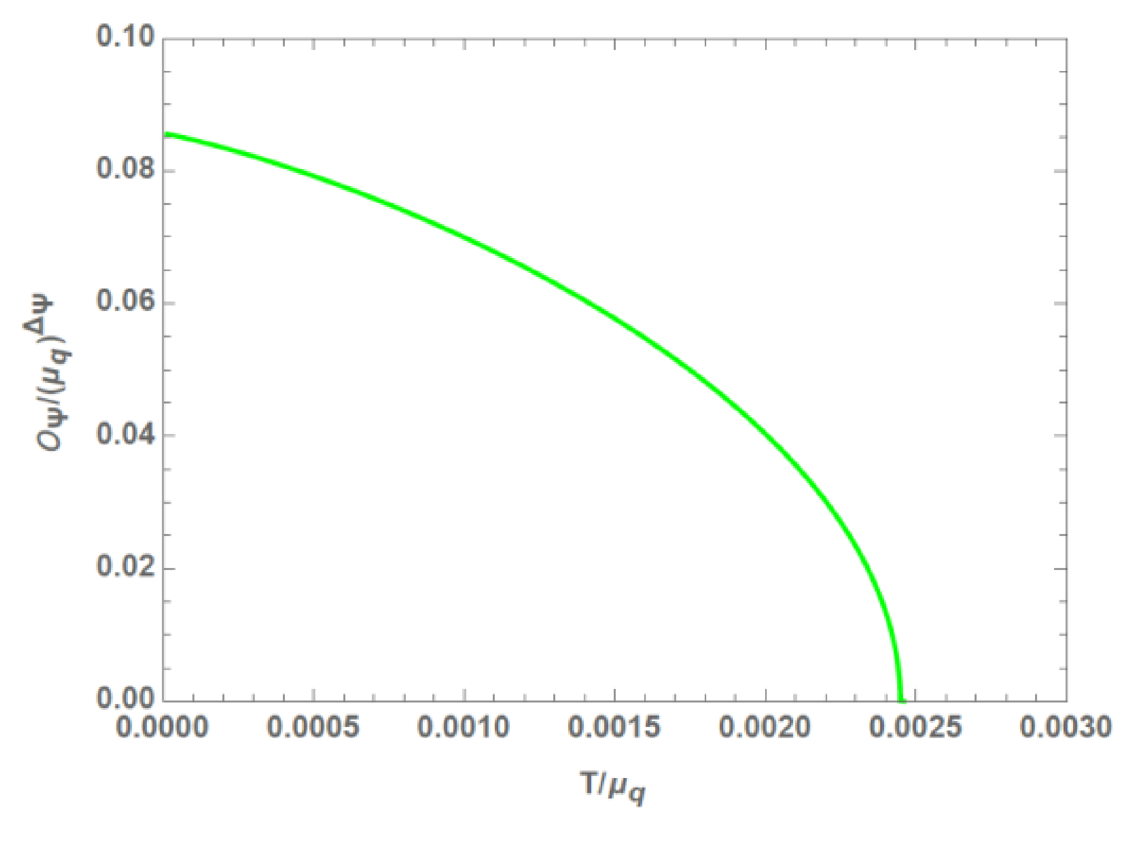

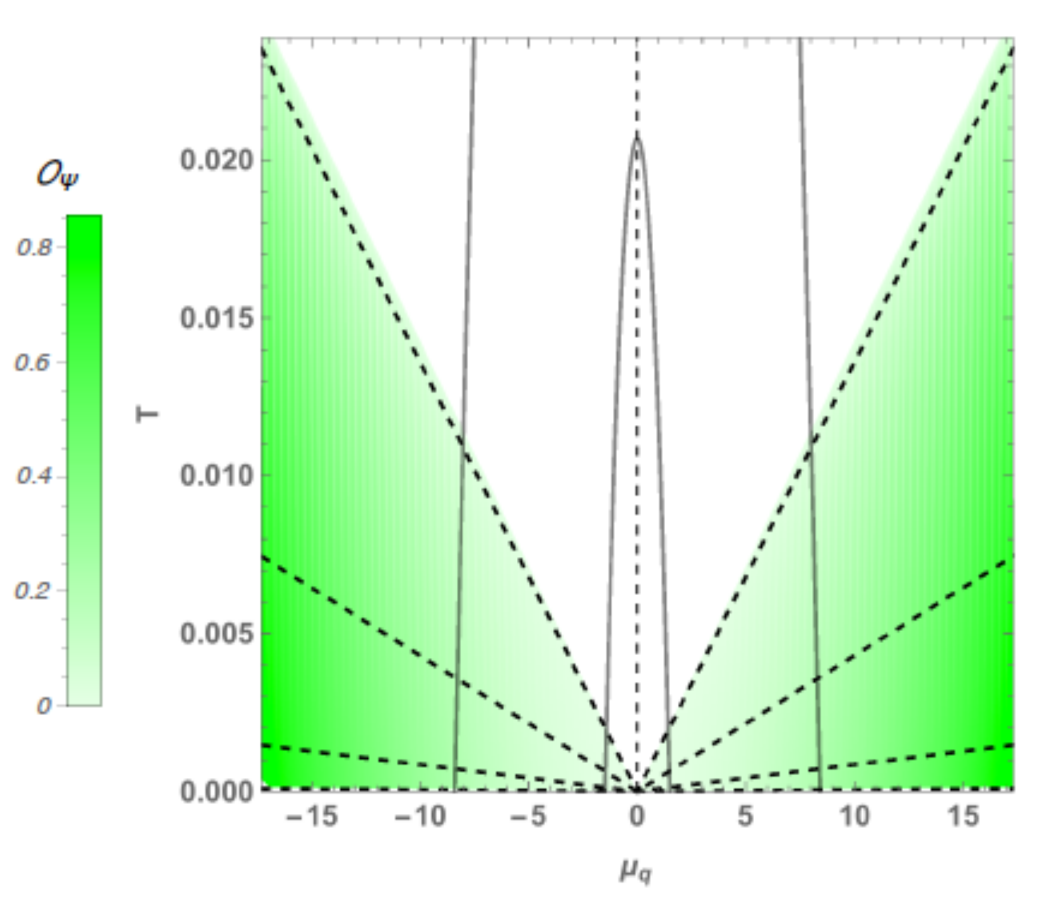

Toy model with critical parameter

$F_1(\phi) = -F_2(\phi) = \phi,$ $m_\phi^2 = -1.5, \quad \lambda_\phi = 0,$ $m_i^2 = -1.5, \quad \lambda_i = 2, \quad i = 1, 2,$

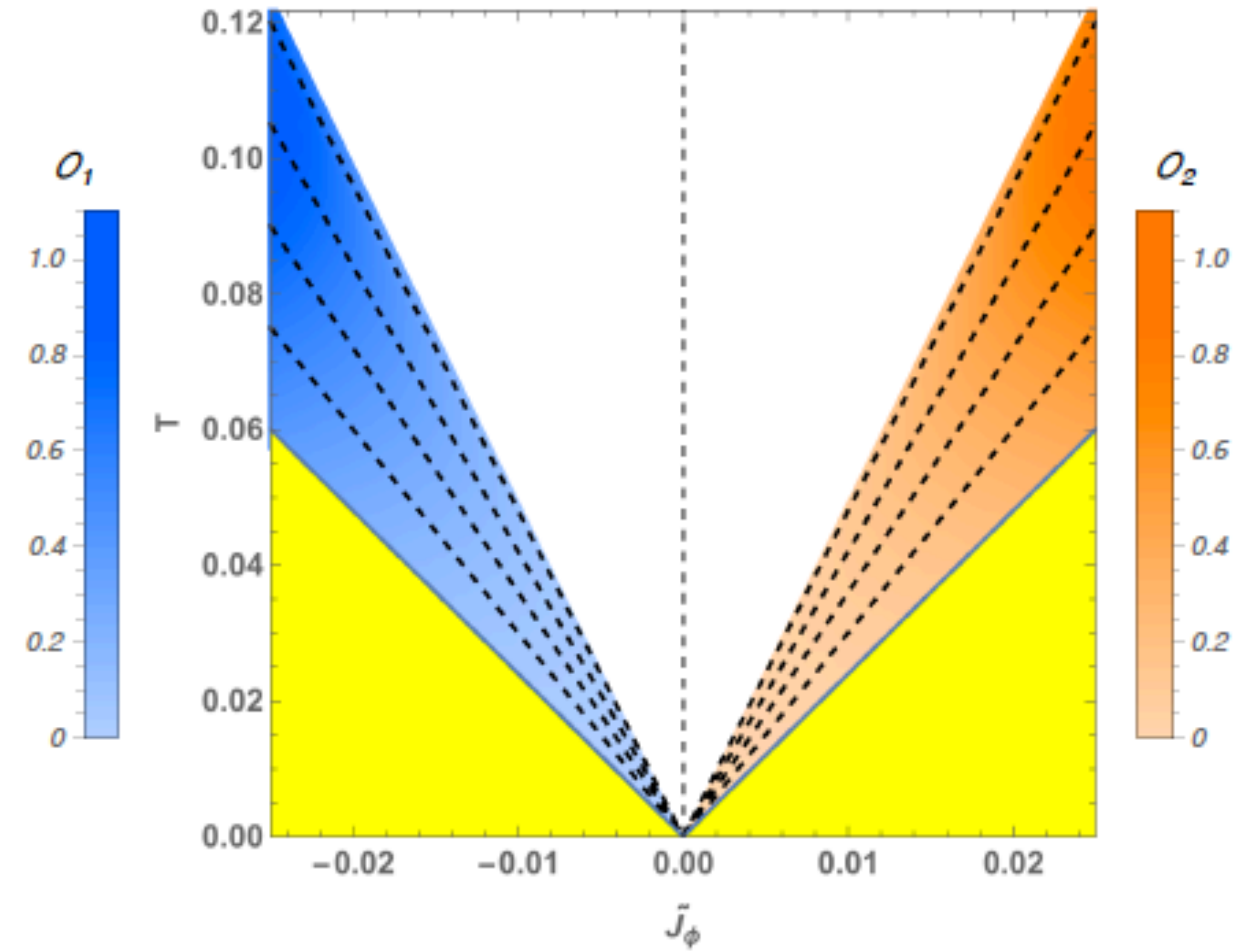

Figure 7: The phase diagram of our test model with the Lagrange density in equation (13) and parameters in (36) and (37). It is the density plot of phase 1(blue) and phase 2 (orange) with coupling functions $F_1(\phi) = -F_2(\phi) = \phi$. We have taken $(T/\mu_q) \simeq 2.76 \times 10^{-4}$ and the notation $\tilde{J}_\phi \equiv (\mathrm{Sign}[J_\phi])|J_\phi|^{1/\Delta_\phi^-}$. The yellow regions are due to numerical unstable.

Model I: Positive doping

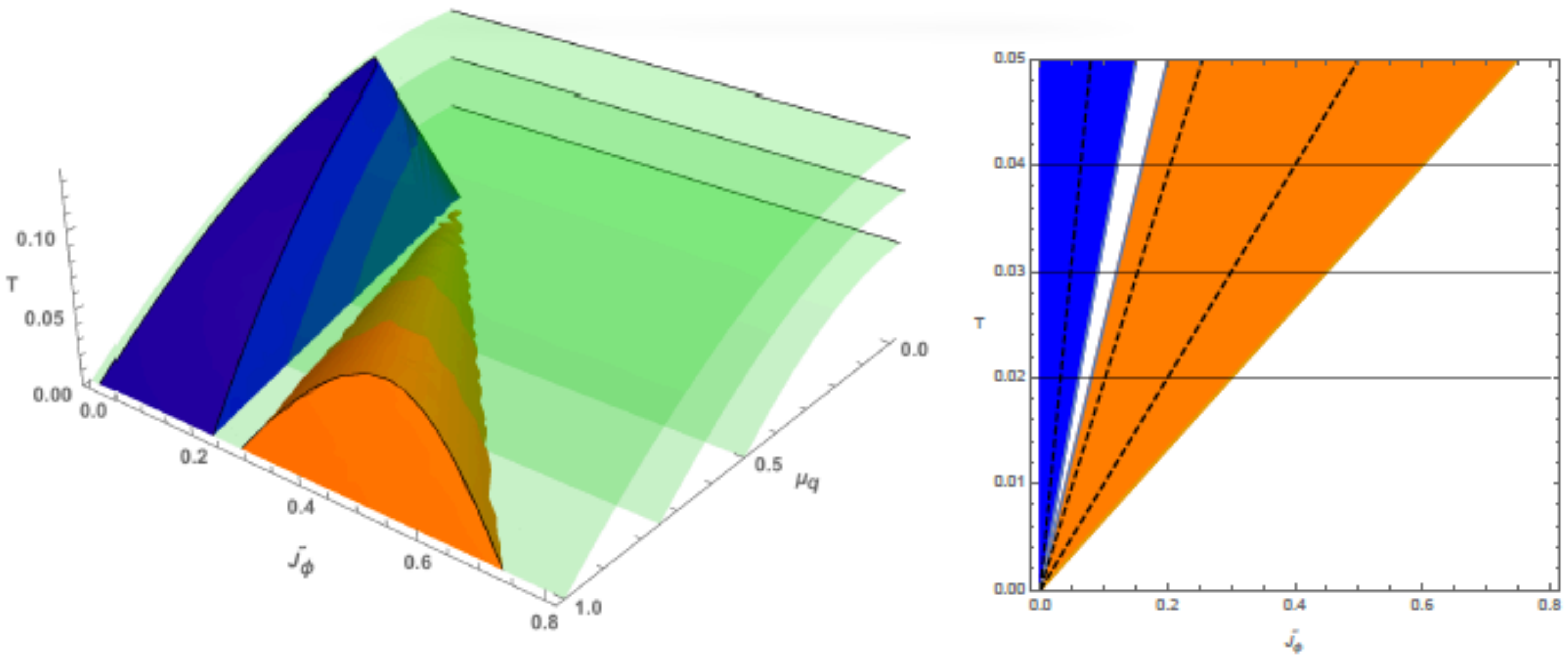

Figure 9: Left: the 3D schematic diagram of Figure 2 in terms of $\{\mu_q, \tilde{J}_\phi, T\}$, where the blue and orange region correspond to ordered phase 1 and phase 2. Three light green surfaces indicate parameter constraint of constant r_h; Right: T vs. $\tilde{J}_\phi$ diagram with a fixed μ_q/T. The dashed line indicate the scalings, and the solid gray line indicate parameter constrain of constant r_h.

Model II: Dome around Critical Point

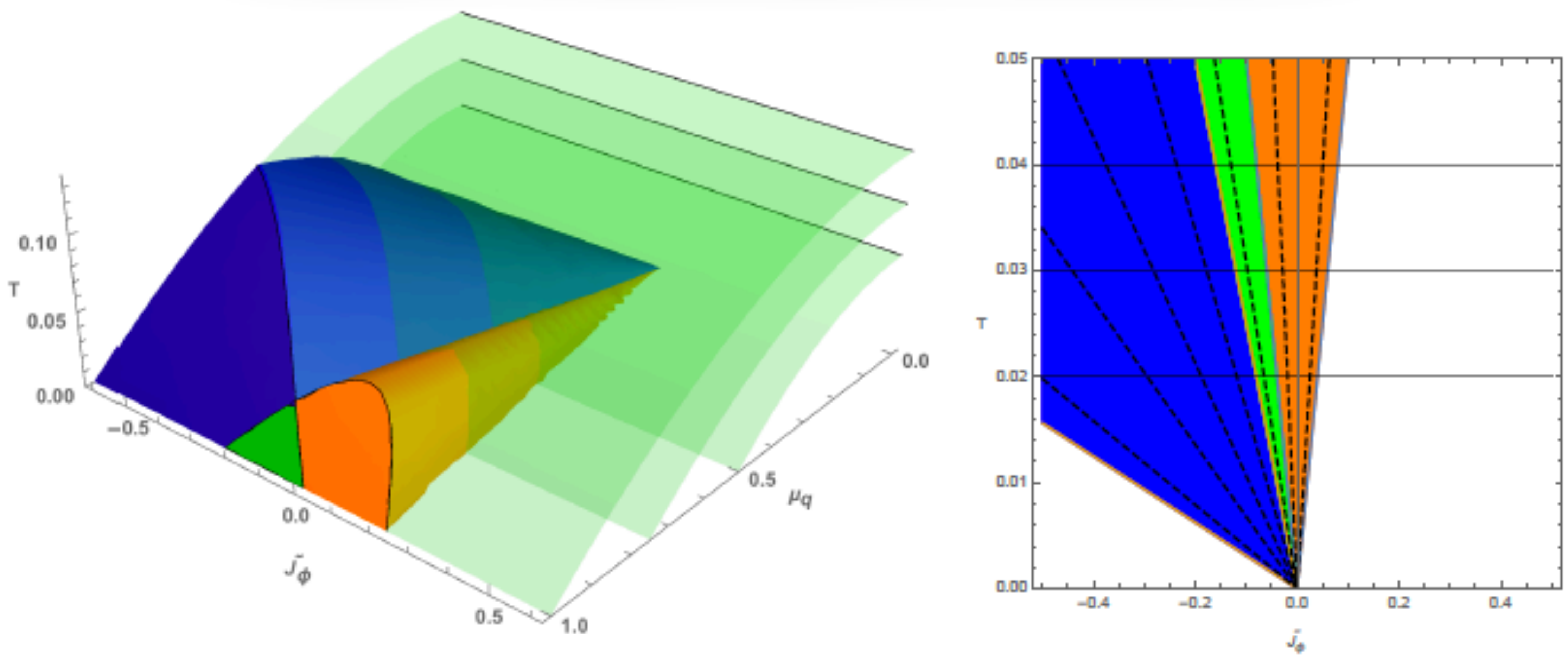

Figure 10: Left: the 3D schematic diagram of Figure 4 in terms of $\{\mu_q, \tilde{J}_\phi, T\}$, where the blue, orange and green region correspond to ordered phase 1, phase 2 and the overlap phase. Three light green surfaces indicate parameter constrain of constant r_h; Right: T vs. $\tilde{J}_\phi$ diagram with a fixed μ_q/T. The dashed line indicate the scalings, and the solid gray line indicate parameter constrain of constant r_h.

Summary & Discussion

A minimal holographic model with dome
Scaling symmetries the the whole Phase

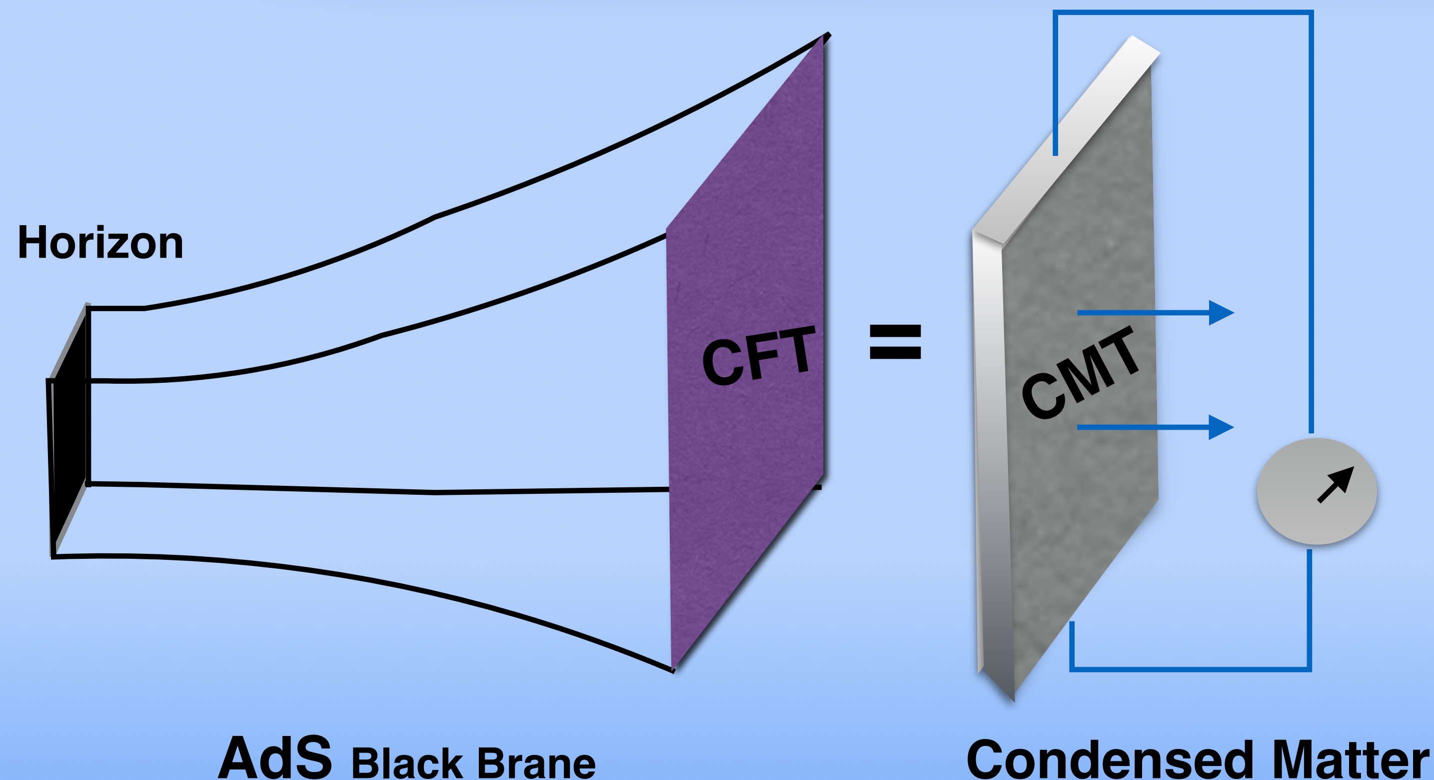

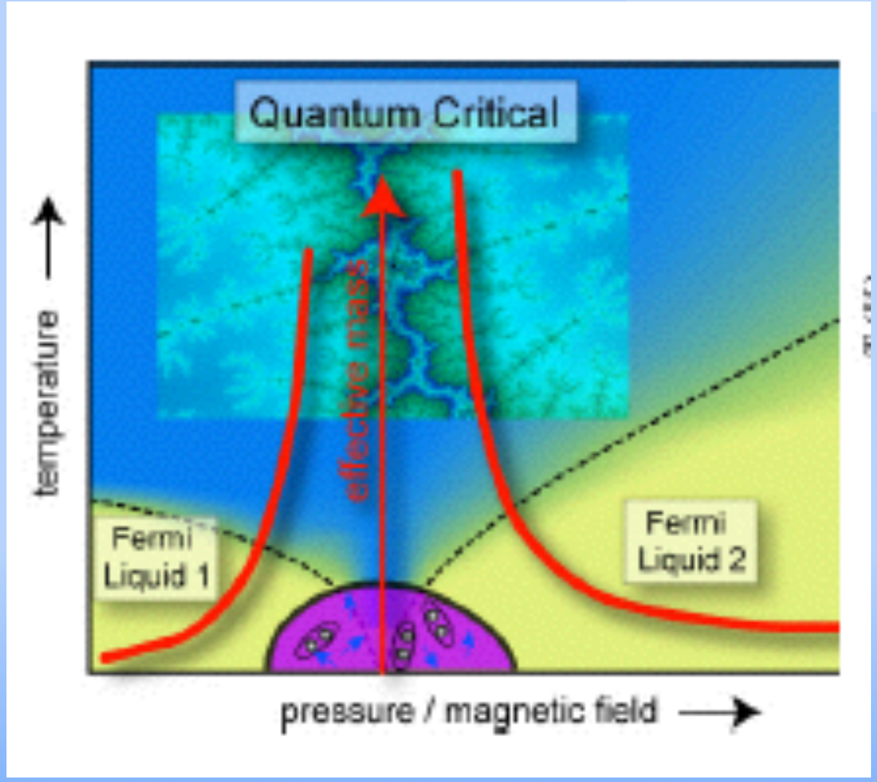

Thanks for your attention!

— zhangyunlong001@gmail.com